de Felice, G., De Santis, S., Garmendia, L. et al. *Mortar-based systems for externally bonded strengthening of masonry*. **Materials and Structures** 47, 2021–2037 (2014). This version of the article has been accepted for publication, after peer review (when applicable) and is subject to Springer Nature's AM terms of use, but is not the Version of Record and does not reflect post-acceptance improvements, or any corrections. The Version of Record is available online at: https://doi.org/10.1617/s11527-014-0360-1

MORTAR-BASED SYSTEMS FOR EXTERNALLY BONDED STRENGTHENING OF MASONRY

Gianmarco de Felice[1,*], Stefano De Santis[1], Leire Garmendia[2], Bahman Ghiassi[3], Pello Larrinaga[2], Paulo B. Lourenço[3], Daniel V. Oliveira[3], Catherine G. Papanicolaou[4]

[1] Department of Engineering, Roma Tre University, Rome, Italy
[2] Tecnalia Research & Innovation, Bilbao, Spain
[3] Department of Civil Engineering, ISISE, University of Minho, Guimaraes, Portugal
[4] Department of Civil Engineering, University of Patras, Patras, Greece

**** Corresponding author:***
E-mail: gianmarco.defelice@uniroma3.it
Telephone: +39.06.5733.6268
Fax: +39.06.5733.6265

ABSTRACT

Mortar-based composite materials appear particularly promising for use as externally bonded reinforcement systems for masonry structures. Nevertheless, their mechanical performance, which may significantly differ from that of fibre reinforced polymers (FRP), is still far from being fully investigated. Furthermore, standardized and reliable testing procedures have not been defined yet. The present paper provides an experimental campaign carried out by laboratories in Italy, Portugal and Spain. The performance of three reinforcement systems made out of steel, carbon and basalt textiles embedded in inorganic matrices has been investigated by means of uniaxial tensile coupon testing and bond tests on brick and stone substrates. The experimental results provide a contribution to the understanding of the structural behaviour of textile reinforced mortars against tension and shear bond stress, and to the ~~design~~ ~~identification~~definition of relevant test procedures.

Keywords: Masonry, Mortar-based composites, Textile reinforced mortar, Tensile tests, Bond tests.

1. INTRODUCTION

An increasing attention has been given in the recent years to the development of innovative technologies based on the use of composite materials for strengthening masonry structures by applying externally bonded reinforcement systems. Recent applications of fibre reinforced polymers (FRP) to vaults, columns and walls have demonstrated their effectiveness in increasing the load-

carrying capacity and in upgrading the seismic strength (Triantafillou and Fardis, 1997; Valluzzi et al., 2001; Corradi et al., 2002; Ascione et al., 2005; Panizza et al., 2008; Grande et al., 2011; Oliveira et al., 2011; Valluzzi et al., 2014). ~~The adoption of I~~inorganic matrices may offer ~~, despite~~ a lower bond strength with respect to FRPs, due to the possible occurrence of weaker failure modes within the reinforcement rather than within the substrate. However, they have ~~has~~ some advantages in terms of overlay-to-substrate compatibility, transpirability, reversibility, fire resistance, cost, and applicability (Papanicolaou et al., 2007; 2008; Cancelli et al., 2007; Carbone and de Felice 2008; Borri et al., 2011; Garmendia et al., 2011; Malena and de Felice, 2014). Moreover, the use of textiles with inorganic matrix seems to be particularly appropriate for application to masonry structures, since the higher bond strength of polymeric matrix cannot be fully exploited because of the low intrinsic mechanical characteristics of the substrate (Aiello and Sciolti, 2006; Oliveira et al., 2011; Garmendia et al., 2012; Grande et al., 2013; Ceroni et al., 2014). Nevertheless, a deeper knowledge needs to be gained for designing mortar-based strengthening systems that are suitable for application to masonry substrates, as well as for identifying their mechanical properties (e.g., under direct tension or shear bond stress) through standardized testing methodologies.

Systemized research on similar systems, such as Textile Reinforced Concrete (TRC), has been conducted by the RILEM TC 201-TRC (Brameshuber, 2006) while ongoing research is currently undertaken by the follow-up TC 232-TDT (Test methods and design of textile reinforced concrete). Despite the fact that the main application target of TRC is integration in new civil ~~works~~ structures rather than strengthening of existing ones, strong analogies exist between mortar-based reinforcement systems and TRC on numerous key issues, including testing methods (Contamine et al., 2011; Hartig et al., 2012), durability and mechanical behaviour. As for the case of tensile behaviour, numerous studies have been carried out (Hegger et al., 2006; Häußler-Combe and Hartig, 2007; Colombo et al., 2013). However, TRC matrices usually consist of high performance finely grained cement concrete, while lime-based mortars might be preferred when strengthening a masonry structure for moisture compatibility reasons and reversibility requirements. As for the reinforcement textiles, beyond those typically used in TRC (glass, carbon or aramid fibre bundles), steel cords (Borri et al., 2011), basalt (Balsamo et al., 2011), and natural fibres (Pacheco-Torgal and Jalali, 2011) may be potentially selected for the strengthening ~~interventions on~~of masonry, provided that fabric layouts are designed to ensure adequate interlocking within a weaker matrix.

In the perspective of using textile reinforced mortar as strengthening system, more research is needed to explore the mortar-based composite-to-substrate bond performance, for which only few contributions have been provided to date, whose preliminary results suggest that significantly lower bond strength and different failure modes may be expected with respect to FRPs (see for instance: Ortlepp et al., 2006; Carbone and de Felice, 2009; D'Ambrisi et al., 2013, Carloni and Subramaniam, 2013).

The present work describes the results of an experimental campaign devoted to the investigation of the mechanical performance of reinforcement systems comprising fibrous textiles embedded in inorganic matrices. The research is currently on-going within the RILEM TC CSM (Composites for sustainable strengthening of masonry). Three research laboratories, affiliated with ~~belonging~~

~~to~~ the University Roma Tre (Rome, Italy, UNIRM3), ~~to~~ with the University of Minho (Guimarães, Portugal, UMINHO), and ~~to~~ with Tecnalia Research & Innovation (Bilbao, Spain, TECNALIA) were involved. The experimental programme comprised Steel Reinforced Grouts (SRG), Carbon Textile Reinforced Mortars (CTRM) ~~with both cement-based and lime-based mortars,~~ and Basalt Textile Reinforced Mortars (BTRM). Both cement-based and lime-based mortars have been used as matrices. The three composite systems were characterised through direct unidirectional tensile tests. Then, the TRM-to-substrate bond performance was investigated using different test setups (~~with~~ single or double lap scheme) and considering various anchorage lengths, substrates (brick and stone), and surface preparation techniques. The work aims at providing a contribution to the understanding of the mechanics of TRM as reinforcing material and to the ~~design identification~~definition of test procedures drawing upon the experience gained from the involved research units.

2. MATERIALS

The properties of the materials used by the three laboratories involved in the experimental campaign are listed in Tables 1 and 2. The former includes the type, compressive strength (f_b, f_m) and the Young's modulus (E_b, E_m) of the substrates and mortar matrices (with subscripts 'b' and 'm' assigned to substrates and mortars, respectively). The tensile strength of the mortar matrices (f_m^t) is also reported.~~, while t~~The latter contains the type, the wire properties (tensile strength, f_{fil}, Young's modulus, E_{fil}, and ultimate strain, $\varepsilon_{u,fil}$), textile properties (tensile resistance, f_t, Young's modulus, E_f, ultimate strain, ε_u and weight, W) and equivalent thickness of the textile (t) used for deriving the stress values. EN 1926 (2006), EN 772-1 (2002), and EN 1015-11 (2007) standards were followed for the tests on natural stones, bricks, and mortars, respectively.

Table 1 Compressive properties of substrates and matrices

Institution			Substrate			Matrix			
Name	Acronym	Country	Type	f_b N/mm^2	E_b N/mm^2	Type	f_m N/mm^2	E_m N/mm^2	f_m^t N/mm^2
Roma Tre University	UNIRM3	Italy	Brick	55.2	16000	Fibre-reinforced cement-based mortar	38.0	15000	7.5
University of Minho	UMINHO	Portugal	Brick	14.2	9500	Lime-based mortar	13.0	14000	
Tecnalia R&I	TECNALIA	Spain	Stone	21.0	5900	Cement-based polymer-modified mortar	22.6	15700	

Table 2 Textile tensile properties

Institution	Type	Filament (1)			Textile				
		f_{fil} N/mm^2	E_{fil} N/mm^2	$\varepsilon_{u,fil}$ %	f_t (2) N/mm^2	E_f (2) N/mm^2	ε_u (2) %	W (1) g/m^2	t (1) mm
UNIRM3	Steel	2474	207000	2.3	2396 (1)	~~190000~~192857	1.61	2110	0.256
	Carbon	4800	240000	1.8	~~3340~~1914	~~238000~~189361	1.~~83~~	168	0.047
UMINHO	Steel	3200	206000	–	3070	190000	1.6	1800	0.227
TECNALIA	Basalt	2100	89000	3.1	–	67000 (1)	–	235	0.035
	Steel	3200	206000	–	3070	190000	1.6	600	0.075

~~All~~ (1) Ddata~~, if not specified otherwise, are~~ provided by the ~~producers~~manufacturers

[42] Data determined experimentally

The mortar used by UNIRM3 was based on a commercially available fibre-reinforced cementitious binder with pozzolanic additives, specifically designed for use in combination with fibre meshes for the reinforcement of masonry structures; the 28-days' compressive strength (derived from 50 mm cubic specimens) and the Young's modulus of the mortar was 38 N/mm^2 and 15000 N/mm^2, respectively. Solid clay bricks were used for bond testing, having a compressive strength of 55.2 N/mm^2 and a Young's modulus equal to 16000 N/mm^2 (derived from compression tests on 50 mm cubic samples). Both steel and carbon meshes were used; the former was a commercial tape-like product consisting of high carbon steel cords unidirectionally oriented (12 cords/inch, which is called by the producer 'medium density'), while the latter was a carbon fibre mesh (more specifically, a textile comprising carbon fibre rovings arranged in two orthogonal directions) made out of textile 4mm wide stripes placed 6mm apart.

Solid clay bricks with dimensions of 200×100×50 mm^3 were used as the substrate for the bond specimens prepared at UMINHO laboratory. The compressive strength of the bricks was characterized through compressive tests ~~carried out according to EN 772-1 (2002)~~ on six 40 mm cubic specimens, in the flatwise direction. A medium density steel mesh (12 cords/inch) was used as the reinforcement inserted in a pozzolanic lime-based mortar matrix (also based on an off-the-shelf dry mix) with 13 N/mm^2 compressive strength (much lower if compared to that used at UNIRM3, which contained cement) and 14000 N/mm^2 Young's modulus. The mortar was characterized by performing compressive tests on five cylindrical specimens with 50 mm diameter and 100 mm height at 28 days.

TECNALIA laboratory used basalt fibre and steel wire meshes. Basalt textile was a grid comprising bitumen-coated fibre rovings arranged along two orthogonal directions. The bitumen coating is typically used in order to enhance the mortar-to-textile bond and, hence, improve certain mechanical properties of the TRM. Basalt textile grid spacing ~~were~~ was 20 mm × 20 mm^2~~.~~, while s~~S~~teel wire fabric had a density of (4 cords/inch~~, low density) was conformed by a polypropylene net, forcing steel fibres to spread in the longitudinal direction~~. A cementitious mortar was used as matrix containing less than 4% of organic resins. After a 28-day curing period, 40×40×160 mm^3 prisms were tested ~~according to EN 1015-11 (2007)~~ to determine the compressive strength and the Young's modulus of the mortar (22.6 N/mm^2 and 15700 N/mm^2, respectively). Stone units were used for bond testing, having 21 N/mm^2 compressive strength and 1300 N/mm^2 Young's modulus.

3. TENSILE TESTS

Despite the ultimate load may be sometimes difficult to be exploited, the tensile behaviour of EBRs may have a certain importance in some structural applications, such as shear reinforcement of masonry panels, extrados strengthening of arches and vaults, and confinement of columns. For this reason, direct tensile tests are required by standard codes (CNR, 2012; ICC, 2013) for the

mechanical characterization of mortar-based reinforcement systems and are expected to become a fundamental step of the industrial process for product qualification purposes.

Direct tensile tests on the different TRM were carried out to in order derive the main mechanical properties of the strengthening systems, such as the tensile strength and stiffness. An overview of the tests performed by the three laboratories involved in the research is shown in Table 3, in which the size of the specimens and the number of textile layers embedded in the mortar are also listed. UNIRM3 performed tests on CTRM and SRG plate specimens having an overall cross section area of 40 mm × 7 mm^2 and a length of 800 mm and 700 mm, respectively. Tests were carried out after 28 days of curing by means of a universal MTS testing machine, equipped with a 500 kN hydraulic actuator, under displacement control at 0.005 mm/s rate (machine compliance < 0.05%). The applied load was measured by a load cell integrated in the testing machine, while the strains were recorded at 10 Hz frequency through four resistive strain gauges (having length of 10 mm and 0.07% precision). Strain gauges were positioned vertically, two per side and parallel to each other, and were applied directly on the fibres, embedded within the mortar layer. For SRG specimens, in order to ensure an accurate measurement of the strain and avoid the detachment of the strain gauge from the steel cords, a small portion of the textile was impregnated with polymeric resin. This was not necessary for CTRM specimens, as the strain gauge and the carbon yarn had approximately the same width (2 mm). The SRG specimens tested at UMINHO had 3 mm mortar cover in each side of the steel cords resulting in total specimen thickness of 6 mm. The specimens' width and length were equal to 50 mm and 450 mm, respectively. Monotonic tests were performed after 28 days of curing using a universal testing machine with a maximum load capacity of 200 kN, under displacement control at 0.033 mm/s constant rate. The applied load was recorded by a load cell integrated in the testing machine, while deformation was monitored by a clip gauge placed mid-height on the specimens. Finally, TECNALIA manufactured specimens with a 100 mm × 10 mm^2 cross section area and 600 mm length. The ends of each specimen were reinforced with two additional layers of textile (extending 200 mm from end to mid-height), in order to promote the failure of the specimen in its middle third portion. Tests were performed on a 100 kN hydraulic testing machine, ~~with automatic~~under displacement control and load measurement precision better than 0.3%. The deformation of the middle third portion was measured by means of two Linear Variable Differential Transformers (LVDT). All the experimental information obtained was recorded using a data logger at 5 Hz frequency.

In the following section on bond tests, it will be shown that in mortar-based EBRs the textile may slip within the matrix, especially when the bond with the mortar is weak (carbon and basalt fabrics in this case). In order to prevent premature debonding by slipping, more layers were placed in the reinforcement. Direct tensile tests have been carried out with the same number of layers used for bond tests.

Table 3 Overview of the direct tensile tests on strengthening systems

Institution	Basalt		Carbon	Steel		Specimen dimension [mm³]
	2 layers	3 layers	3 layers	4 cords/inch	12 cords/inch	
UNIRM3			4			40×7×800
					4	40×7×700
UMINHO					4	50×6×450
TECNALIA	7	7		7		100×10×600

Based on the specific properties of the specimens tested and on available laboratory facilities, ~~D~~different solutions were ~~adopted~~ developed by the three laboratories to ensure adequate clamping of the specimen, which is necessary to guarantee a uniform load transfer and avoid stress concentration in the gripping area (Fig. 1). UNIRM3 chose to leave each end of the specimen free of mortar and to apply aluminium tabs by means of a strong structural glue. Then, the tables were clamped within the wedges of the testing machine. A similar procedure was followed by UMINHO. Finally, TECNALIA gripped the ends of the TRM specimens by means of a mechanical device made out of two steel plates having rough surfaces (knurl); extra textile strip was placed between the steel plates and the specimen.

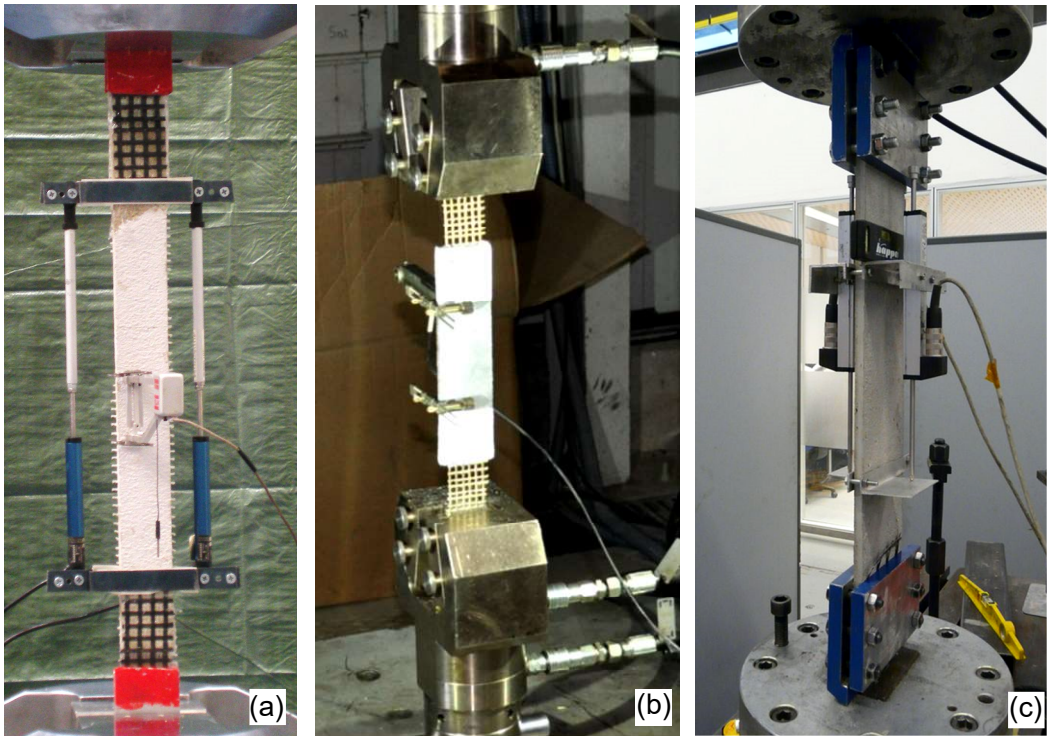

Fig. 1 Setup used for tensile tests by UNIRM3 (a), UMINHO (b) and TECNALIA (c)

The results of tensile tests are shown in Figs. 2, 3 and 4 for SRG, CTRM, and BTRM, respectively. Stress values correspond to the applied resultant load divided by the fibres' area. The latter is ~~(in the direction of loading), being the latter~~ equal to the product of the number of layers, the specimen's width, and the textile design thickness in the direction of loading. The results (per TRM) present a relatively low scatter, especially for what concerns the maximum tensile stress (f_t), despite the differences in specimens' size and setups amongst different laboratories. Based on the present experimental investigation (in which slightly

different setups have been used to test different composites under tension), higher strength values resulted from SRG specimens (in the order of 3000 N/mm^2), while BTRM and CTRM showed similar tensile resistance of about 1200 N/mm^2. The tensile strength of SRG specimens was found to be close to the tensile strength of the textile itself; for BTRM and CTRM specimens, though, a significant reduction was observed. The TRM with fibrous reinforcements (of more than one layers) may exhibit lower tensile strength values than those of the textiles. Misalignment of the textile layers (or of the rovings of the same textile layer), areas in between layers not adequately filled with mortar, wear of fibres at the vicinity of crack edges and nonuniform stress distribution within the textile are some of the reasons why the tensile strength of the composite is generally less than that of the textile itself (Häußler-Combe and Hartig, 2007). Furthermore, according to the producers, this may be related to the mechanical stress induced on basalt and carbon wires in the textile manufacturing process. ~~Finally, a premature specimen failure may occur at its ends due to stress concentrations in the vicinity of the clamping wedges of the testing machine.~~

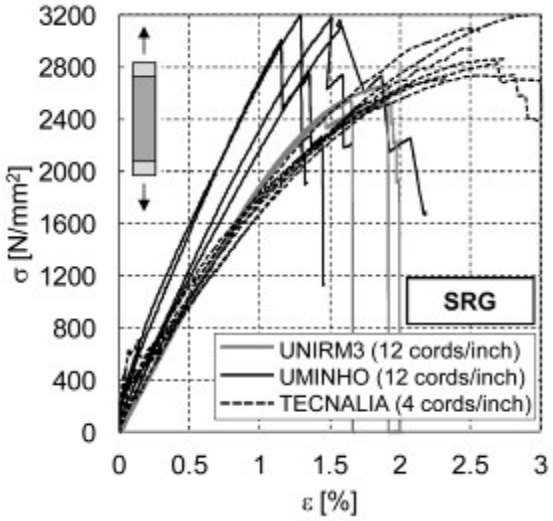

Fig. 2 Stress-strain curves of SRG specimens under uniaxial tension.

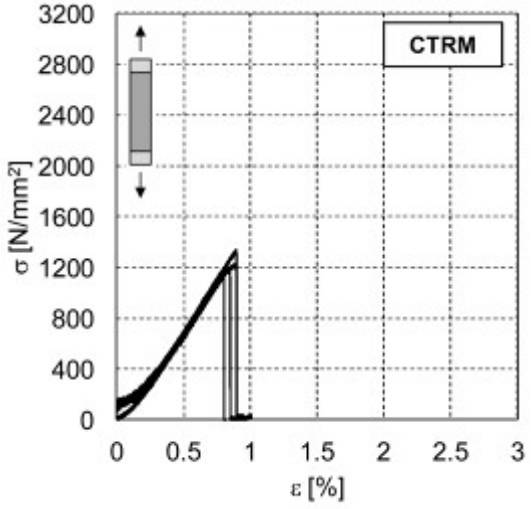

Fig. 3 Stress-strain curves of CTRM specimens under uniaxial tension.

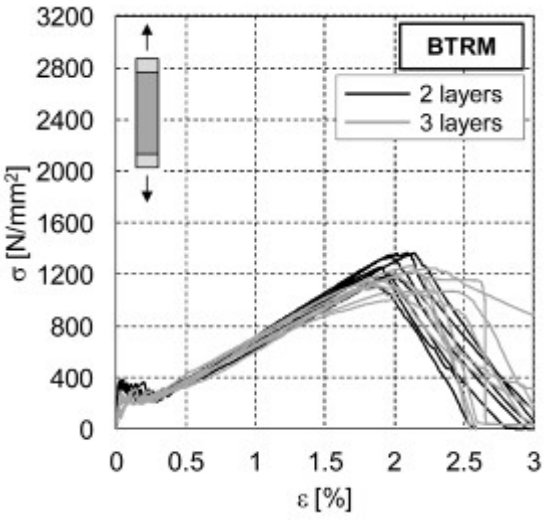

Fig. 4 Stress-strain curves of BTRM specimens under uniaxial tension.

In the present case, the tensile strength and stiffness of basalt TRM was not strongly influenced by the number of layers of textile embedded in the mortar, as shown in Fig. 4. The mechanical properties of mortar seems to affect only the initial non-cracked behaviour (which is clearly visible in Fig. 4 for BTRM specimens), while, once cracking occurs, a slight tension stiffening effect takes place without significant changes in the tensile strength of the composite. Conversely, the mortar plays a very important role in the bond mechanism as shown in the next section.

As for the ultimate strain (ε_u), i.e., the strain corresponding to the maximum stress, it was between 1% and 2% for SRG with higher density (12 cords/inch) and about 2.5-3% for SRG with lower density (4 cords/inch), about 0.8% for CTRM and, finally, about 2% for BTRM. The latter also showed a lower stiffness of about 6×10^4 N/mm^2, which is clearly related to the lower Young's modulus of the basalt filaments.

The three characteristic response stages of textile reinforced mortar (or concrete, as it is also termed) under uniaxial tensile loading (Brameshuber, 2006; Cuypers and Wastiels, 2006) are also observable on the stress-strain curves, especially for BTRM specimens. The first state corresponds to the behaviour of the uncracked specimen. When the tensile strength of the mortar is reached the first crack is formed and the second stage, the multiple cracking one, starts. The length of the multiple cracking stage was reduced with a higher number of reinforcement layers, as also observable in reinforced concrete (Cuypers and Wastiels, 2006). In the third stage (post-cracking stage during which the crack pattern has been stabilized), the composite is stressed up to the strength of the textile. The stiffness of the post-cracking stage was found to be lower than that of the textile if loaded independently; this is also reported by other studies (Brameshuber, 2006) and it is attributed to the premature failure of some filaments and to the premature debonding of either the core filaments (for textiles with uncoated rovings) (Ohno and Hannant, 1994) or the coated rovings. When the remaining filaments cannot bear the applied load, their fracture causes the whole composite to rupture. As shown in Figs. 2-4, failure of SRG specimens occurred as a progressive rupture of the cords, after a clear loss of linearity in the stress-strain response curve. CTRM specimens displayed a brittle failure of the

entire textile while in BTRM specimens some sort of progressive (although very fast) deterioration is visible in the post-peak branches of the stress-strain curves, which may be related to the textile unravelling within the matrix. ~~Nevertheless, a slight slippage of the specimen's ends within the clamping wedges of the testing machine may occur at this stage of the test~~The fundamental difference in the tensile behaviour of SRG with respect to CTRM and BTRM depends on the different structures of the reinforcement textiles. Steel cords are homogeneous and interact with the matrix at their perimeter, while carbon and basalt textiles are made out of bundles of filaments~~.~~, such that only the external filaments directly interact with the mortar matrix, while the load transfer to the core ones relies on the bond between filaments. A bond failure between filaments within a bundle (telescopic rupture) may be responsible of larger displacements in CTRMs and BTRMs (Mobasher et al., 2006).

The results of all tensile tests are presented in Table 4, in which the elastic modulus (E_t) of the TRM specimens was obtained between stress values corresponding to 30% and 60% f_t, during the last stage (cracked specimen). ~~At this stage, the TRM is working as a composite material since the cracking of the specimen allows the load transfer to the whole composite.~~ At this stage, despite the matrix is cracked, the specimen is still working as a composite as the mortar between consecutive cracks provides both a stiffening effect and a load redistribution amongst the yarns/cords of the textile. ~~When available~~At UNIRM3, in addition to global displacements, ~~the~~ local strains ~~measurements~~ were ~~based on the recordings of the~~recorded by resistive strain gauges, placed directly on the textile~~,~~ (within the mortar), to avoid the influence of crack development on the acquired data and derive local measures in the middle portion of the specimen.

Table 4 Mean values of the results of tensile tests (standard deviation in brackets)

Reinforcement	Institution	f_t [N/mm^2]	E_t [N/mm^2]	ε_u [%]
SRG	UNIRM3	2558 (7.4%)	209805 (4.9%)	1.90 (13.2%)
	UMINHO	3134	217500	1.37
	TECNALIA	2959	150400	2.76
CTRM	UNIRM3	1191 (8.9%)	196525 (7.0%)	0.74 (9.5%)
BTRM (2 layers)	TECNALIA	1256	59000	1.96
BTRM (3 layers)	TECNALIA	1195	57000	2.10

Independently from the type of textile used, and from the mortar adopted as matrix, the crack development observed during tensile tests on -TRM specimens was characterized by the presence of cracks transversal to the direction of the applied load, clearly identifiable in the response curves and visible during testing at low stress values. The crack spacing and width were dependent on the type and quantity of reinforcement and on the te~~ns~~xtile-to-matrix bond behaviour. Higher fibres' volume fractions, as well as fibres with higher stiffness, gave rise to denser crack patterns. A larger number of narrow cracks developed in SRG specimens, which may be related to a better interlocking between the steel cords (of uneven surface as they are made by twisting steel filaments) and the mortar. Improved bond conditions hinder slipping of the textile within the mortar and the development of few wide cracks. Transversal cracks sometimes developed in the vicinity of the aluminium tabs used to grip the samples (Fig. 5a), highlighting the importance of clamping in tensile testing. However, this was not evident for SRG

specimens (Fig. 5b), probably due to the higher toughness of the material, and for BTRM specimens, where the end of the specimens were strengthened and cracks only appeared in their middle third (Fig. 6).

Fig. 5 Damage pattern in tensile tests: development of cracks in the vicinity of the aluminium plates in CTRM (a) and detachment of the mortar in SRG (b)

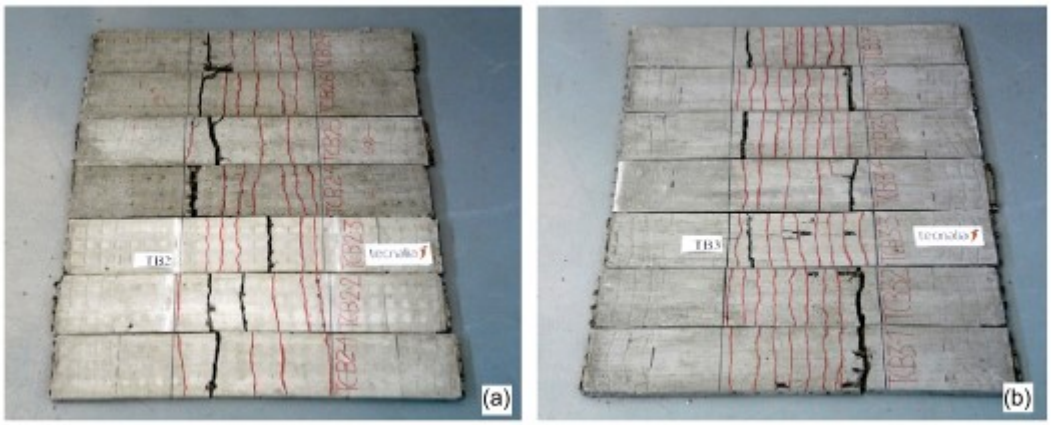

Fig. 6 Tensile tests on BTRM: development of the crack pattern in the middle third of the specimens on series TB2 with 2 layers (a) and TB3 with 3 layers (b)

4. BOND TESTS

4.1. Experimental programme and test setup

Tests on bond performance of TRM were carried out on brick and stone substrates. Brick units were tested by UNIRM3 and UMINHO with CTRM and SRG reinforcements, while stone units were used by TECNALIA to test BTRM reinforcements. An overview of the testing programme is given in Table 5. A standard wet lay-up procedure was followed to bond the steel, carbon or basalt

textile sheets on either solid clay brick or stone substrates. The procedure involved the application of a 2-3 mm thick mortar layer on the block's surface (smoothing out any surface irregularities) and the subsequent bonding of the textile by hand and roller pressure. The textile was pressed slightly into the fresh mortar, which protruded through all the perforations between fibre rovings. The mortar was also applied in between layers (where applicable) ~~at a thickness of 2-3 mm~~ and on top of the last textile layer. The total ~~at a~~ thickness ~~of~~ was 6-7 mm. The bond with the mortar matrix in carbon and basalt fabrics is weaker than in SRG, so premature slipping may occur. In order to prevent this kind of rupture, at least for short anchorage lengths, more layers of carbon and basalt were used. Curing of the TRM overlays was achieved in room conditions (about 15-20°C and 50-60% R.H.). More information regarding surface preparation techniques followed for specimens employing brick substrates will be given further on in the text.

Table 5 Bond testing programme

~~Institution~~	Fibre	Basalt (2 layers)	Carbon (3 layers)		Steel (1 layer)	
	Setup	SL	DL1	DL2	SL	DL2
~~UNIRM3~~	Brick		6	8		12
~~UMINHO~~	Brick				8	
~~TECNALIA~~	Stone	9				

Aiming at avoiding the fibre rupture and focussing on bond performance, 2 layers of basalt and 3 layers of carbon were applied. As for steel, textiles made out of galvanized steel cords were used: one with 4 cords/inch (low density textile) and one with 12 cords/inch (medium density textile).

Drawing on previous experience on FRP (Valluzzi et al., 2012), four different shear bond testing setups were used: two single-lap (SL) and two double-lap (DL1 and DL2), as shown by Figs. 7 and 8. Very similar single-lap test schemes were used by UMINHO and TECNALIA, consisting of stiffened steel plates welded so as to form an angle of 90° (Fig. 7). At UMINHO, the specimens were supported appropriately to avoid misalignments in the load application and were loaded from above (Fig 7a). Tests were carried out under displacement control at a rate of 0.005 mm/s. The load was measured by a load cell while the ~~global~~ slip between the reinforcement and the brick was measured by means of two LVDTs mounted at the loaded end. At TECNALIA, the specimens rested on the bottom of the steel frame and the reinforcement sheet was loaded from below (Fig 7b). Tests were performed using a 5 kN Lloys Universal Testing machine under displacement control at 0.008 mm/s rate. Displacements were measured by LVDTs located on both bonded and unbonded areas of the reinforcement.

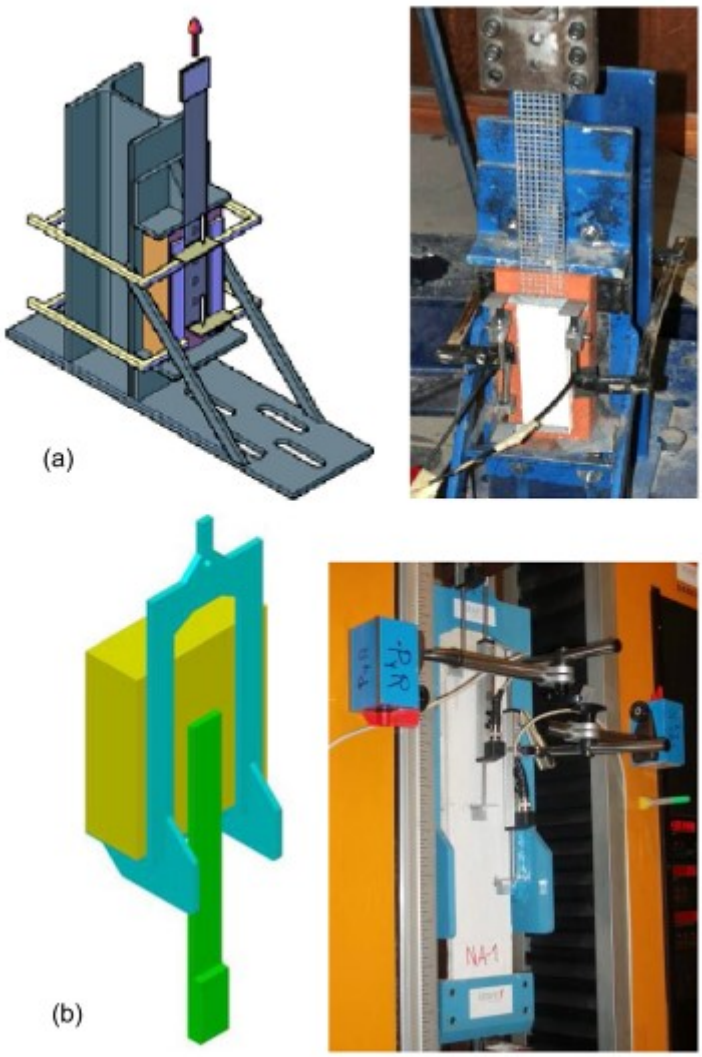

Fig. 7 Single-lap (SL) setup for bond shear tests carried out at UMINHO (a) and TECNALIA (b)

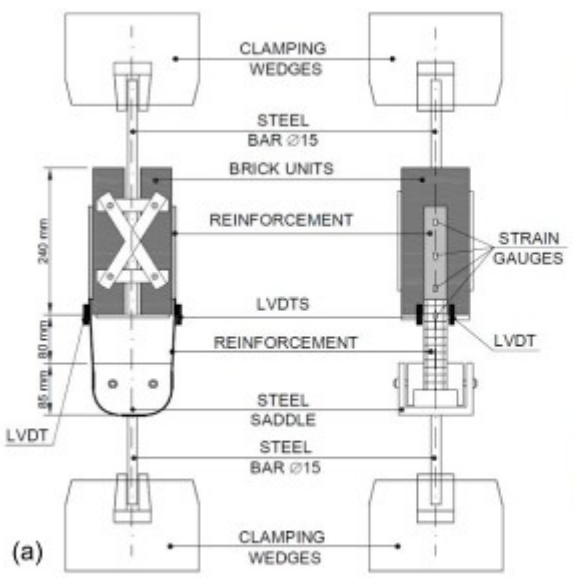
CLAMPING WEDGES
STEEL BAR Ø15
BRICK UNITS
REINFORCEMENT
STRAIN GAUGES
240 mm
LVDTS
LVDT
REINFORCEMENT
80 mm
85 mm
STEEL SADDLE
LVDT
STEEL BAR Ø15
CLAMPING WEDGES
(a)

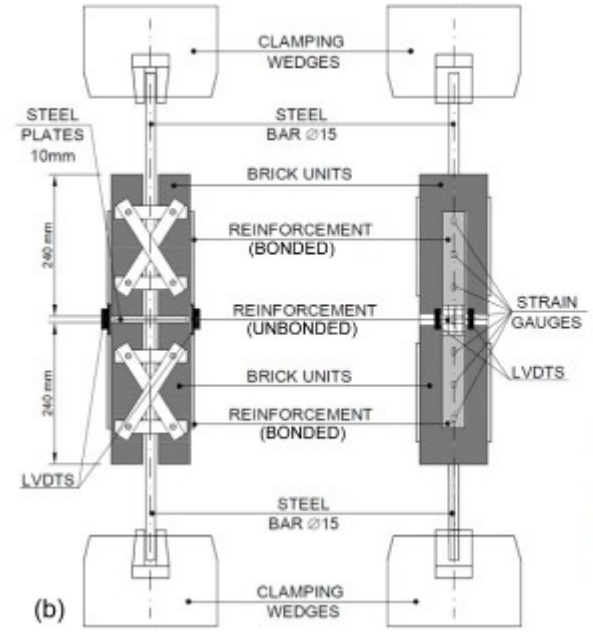
CLAMPING WEDGES
STEEL PLATES 10mm
STEEL BAR Ø15
BRICK UNITS
240 mm
REINFORCEMENT (BONDED)
REINFORCEMENT (UNBONDED)
STRAIN GAUGES
LVDTS
240 mm
BRICK UNITS
REINFORCEMENT (BONDED)
LVDTS
STEEL BAR Ø15
CLAMPING WEDGES
(b)

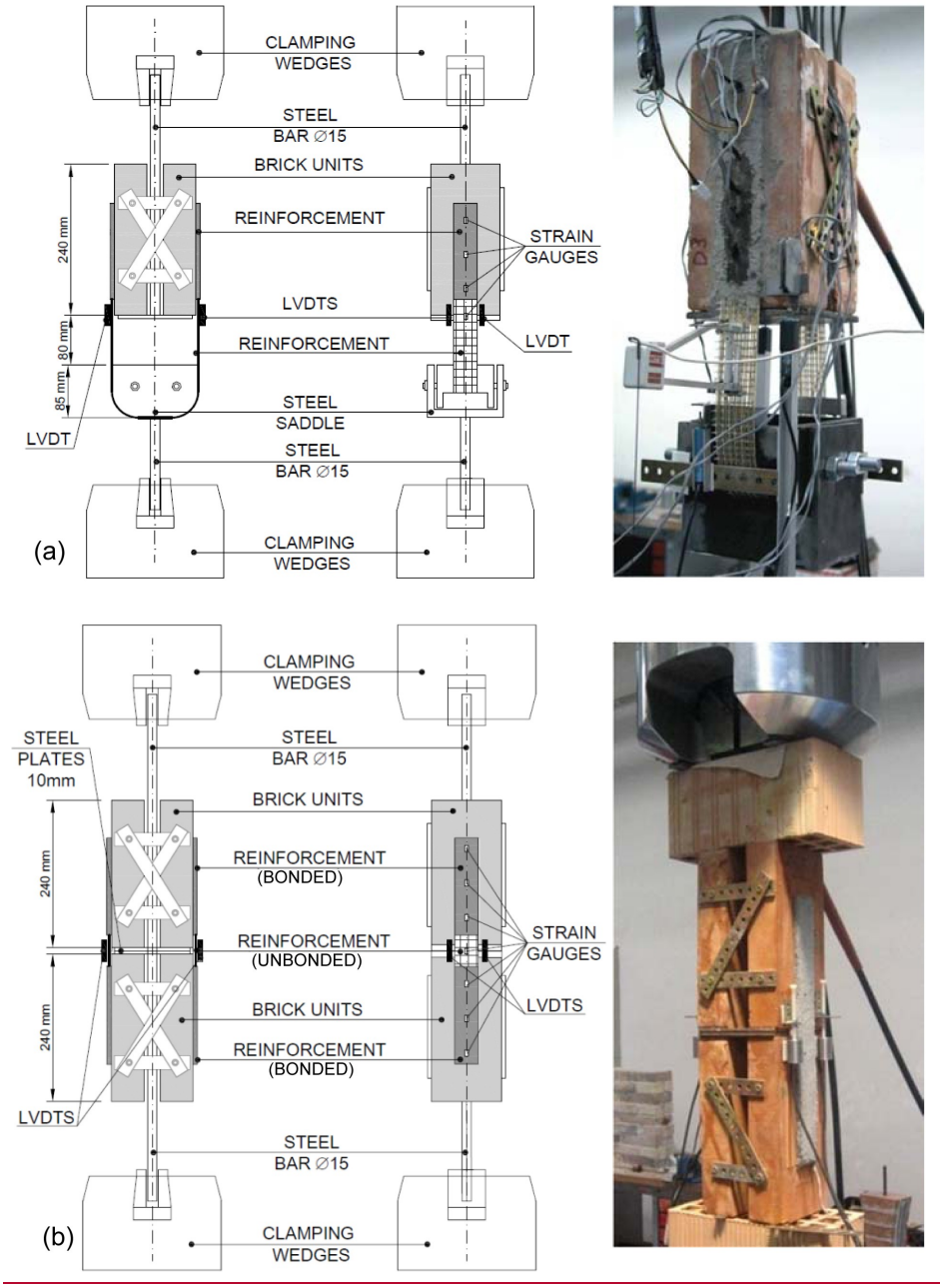

Fig. 8 Double lap setup for shear bond tests: type 1 (DL1, a) and type 2 (DL2, b)

UNIRM3 used double lap setups (DL). Specimens were built by joining together two bricks, placed parallel to each other at a pre-established distance, by means of steel plates; the reinforcement was then applied on both external faces. Setup DL1 (Fig. 8a) consisted of two or four bricks (depending on the anchorage length) pulled by the testing machine in one direction (upwards in the present case) through a steel bar welded to a steel plate (on which the bricks rested), while a continuous U-shaped reinforcement strip was pulled in the other direction (downwards) by means of a semi-circular steel saddle, having a diameter equal to the specimen width (1301 mm) so as to apply pure shear stresses on the brick-reinforcement interface. In test set-up DL2 (Fig. 8b) specimens were made out of four bricks. Two bricks were pulled upwards while the other two were pulled downwards by the testing machine. Two separate strengthening strips were applied on the external faces so as to connect two bricks by crossing the gap

between them. In UNIRM3 tests were performed by using a 500 kN MTS Universal Testing machine under displacement control at 0.005 mm/s rate. The load was recorded by a load cell integrated in the testing machine, while four LVDTs with 10mm stroke and 0.05 mm sensitivity were used to record relative displacements between reinforcement sheets and brick substrate. Finally, a set of 2.5 mm long strain gauges was also applied directly on the fibres (embedded in the matrix), with regular distance between each other, on both sides of the specimen to record local strain values along the reinforcement strip. Furthermore, a reinforcement band was left unbonded for a length of 10mm from the tip of the sample in order to avoid local stress concentrations induced by boundary effects.

Aiming at investigating the effect of the anchorage length on the ultimate load and at detecting information on the effective anchorage length (defined as that necessary for a complete stress transfer between reinforcement and substrate), various anchorage lengths were used, ranging from 55mm to 440 mm. More specifically, UNIRM3 tested the bond performance of SRG with 55 mm, 110 mm and 220 mm and CTRM with 55 mm, 220 mm and 440 mm for a total of 12 tests on SRG and 14 on CTRM; for these specimens bricks were used as a substrate. At UMINHO, a single anchorage length of 150 mm of SRG bonded on bricks was adopted with two different substrate preparation techniques; the first was minimal and involved cleaning and dusting the brick's surface while the second employed by sand-blasting. Finally, TECNALIA tested 9 stone specimens reinforced with BTRM with an anchorage length of 85 mm, 150 mm and 220 mm.

The experimental investigation made it possible to detect the TRM-to-substrate shear bond failure mode for the different textiles and anchorage lengths investigated as well as to derive the global response in terms of load vs. displacement relationships. Finally, the strain profile along the reinforcement strip, ~~derived~~ recorded for SRG specimens, gave some indication on the activation and propagation of the debonding phenomena and on the effective anchorage length.

4.2. Failure modes

Three failure modes were observed: debonding at substrate-matrix interface with peeling off of the brick surface (a), debonding at the textile-matrix interface (b) and slipping of the cords or rovings from the matrix (c), as sketched in Fig. 9. In the latter case the weak surface is the interface between the cords or rovings of the reinforcement textile and the mortar matrix they are embedded in.

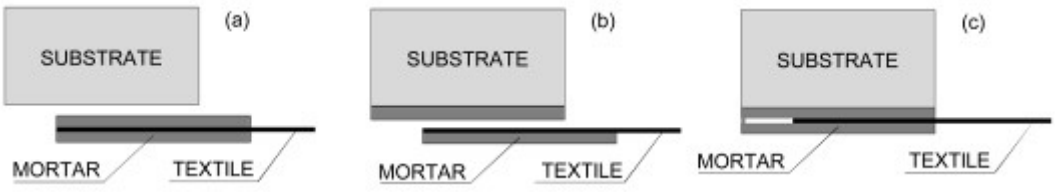

Fig. 9 Failure modes: debonding at substrate-matrix interface and peeling of the brick surface (a), debonding at fibre-matrix interface (b) and slipping of the textile from the matrix (c)

Differently from strengthening systems based on polymeric resins, mortar-based systems generally suffered a concentrated failure within the reinforcement layer, without extending the damage into the substrate. In SRG specimens the first

failure mode (a) generally occurred with the shortest (55 mm) anchorage length (Figs. 10a,b); this observation comes into agreement with the findings of previous experimental studies on concrete (Matana et al., 2005), thus indicating that shorter anchorage lengths may induce higher stresses in direction normal to the mortar-substrate interface, due to the misalignment between this surface and the textile embedded in the mortar matrix. These normal stresses are responsible of the extraction of aggregates from the grout (ripping) observed in the failure mode of specimens with shorter anchorage lengths. On the contrary, a brittle failure by debonding at the textile-matrix interface (b) was observed with the longest anchorage lengths (220 mm and 440 mm), as shown in Figs. 10c,d. Finally, it should be considered that different failure modes may be associated to different effective anchorage lengths as failure occurs on different surfaces. The effective length of failure mode (a) is likely to be shorter than that of mode (b). ~~However~~ The results of the tests performed on SRG showed that the surface preparation may significantly affect the failure mode. In the brick specimens with minimal surface preparation, the mortar detached from the brick surface (failure mode a, Fig. 11a), while steel cord slipping with mortar cover separation was observed in the sand-blasted specimens, for both short and long anchorage lengths (combined failure mode b-c, Fig. 11b).

Similarly, debonding at the substrate-mortar interface was observed in stone specimens reinforced with BTRM with shorter anchorage lengths (85 mm), accompanied by the appearance of transversal cracks also in the unbounded portion of the reinforcement (Fig. 12a). On the contrary, the development of transversal cracks outside the bonded area occurred with the longest anchorage lengths (150 mm and 220 mm); the slipping of the fibres within the mortar matrix is clearly visible in Fig. 12b. As fibres and mortar matrix are subjected to the same elongation outside the bonded area due to equilibrium, such transversal cracks can only develop once the transfer of shear stresses between the substrate and the matrix and between matrix and fibres occurs, inducing the slipping of the textile within the mortar (failure mode c) to be activated before the other failure mechanisms.

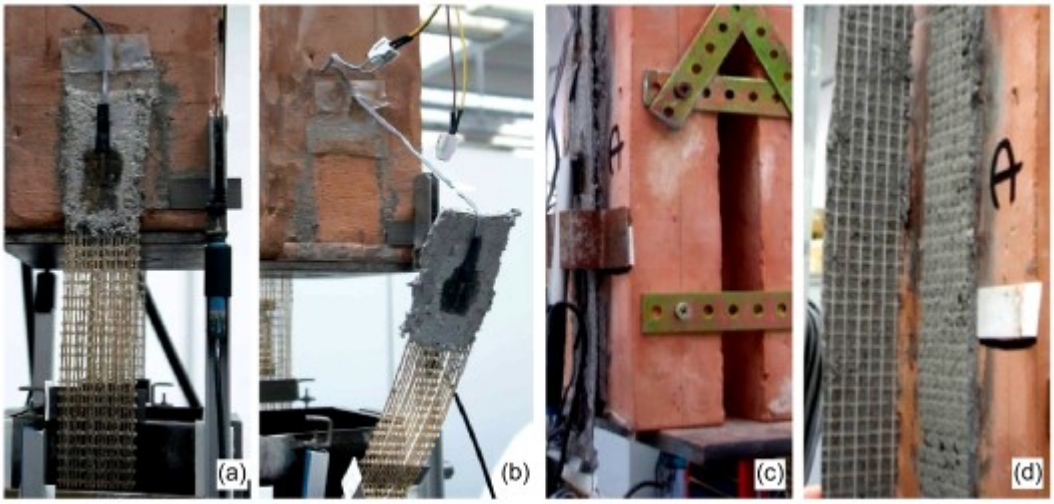

Fig. 10 Failure modes in SRG specimens with different anchorage lengths: debonding at substrate-matrix interface in specimens with anchorage length 55 mm (a, b) and at the textile-matrix interface in specimens with anchorage length 220 mm (c, d). (all specimens received the same minimal surface preparation prior to SRG application)

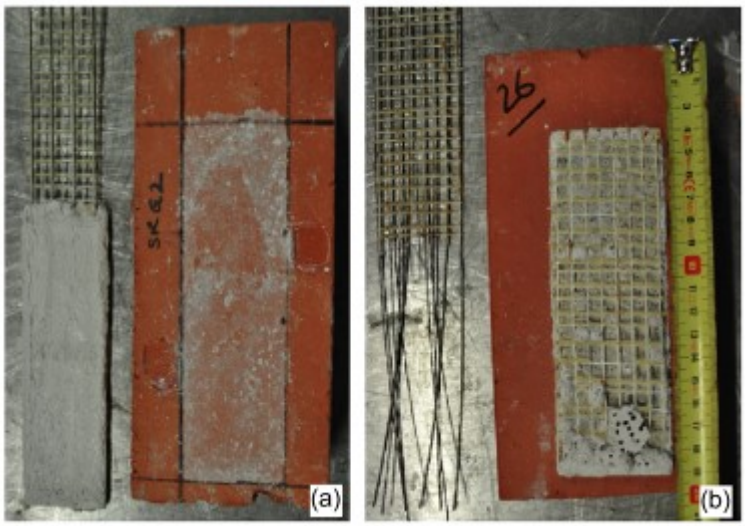

Fig. 11 Failure modes in SRG specimens with different surface preparations: specimens with minimal surface preparation (a) and specimens with sand-blasted surface (b)

Fig. 12 Failure modes in BTRM specimens: debonding at the substrate-matrix interface in specimens with anchorage length 85 mm (a) and slipping of the fibre rovings from the matrix in specimens with anchorage length 220 mm (b)

In CTRM specimens, the fibre-matrix interface generally resulted to be the weakest element; sliding of the fibre within the matrix (failure mode c) was observed in the specimens with the shortest anchorage lengths (55 mm and 110 mm), as shown by Figs. 13a,b while debonding at the fibre-matrix interface occurred for the longest one (220 mm), respectively. Intermediate anchorage lengths (165 mm) gave rise to a combined failure mode consisting in an initial partial debonding of the matrix until the development of a transversal crack, and in the subsequent sudden sliding of the fibre within the matrix inducing a brittle failure (Figs.13c,d).

The failure modes displayed by all the samples of the present experimental campaign are indicated in the next section.

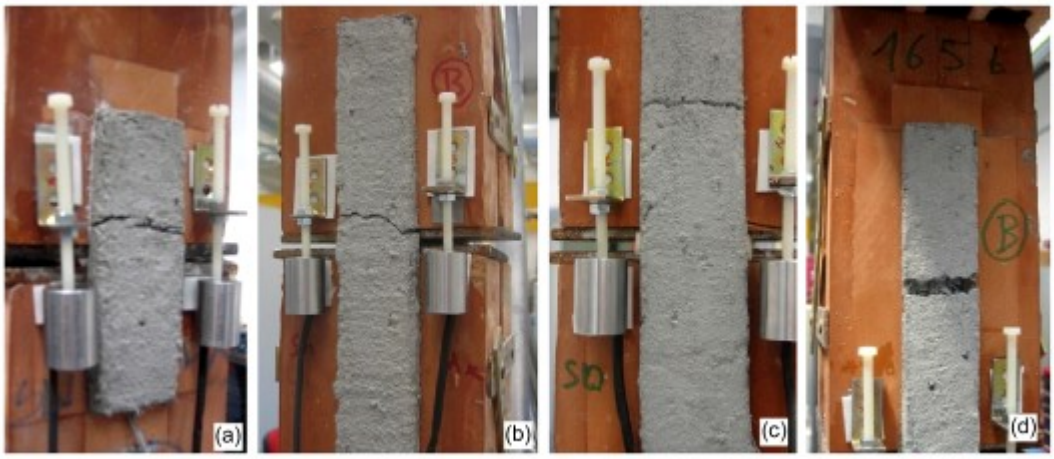

Fig. 13 Failure modes in CTRM specimens: slipping of the fibre rovings from the matrix in specimens with anchorage length 55 mm (a) and 110 mm (b) and combined failure with initial debonding of the matrix and subsequent slipping of the fibre rovings from the matrix in specimens with anchorage length 165 mm (c, d)

4.3. Results

The global response of the reinforcement-substrate systems under shear loads is represented by F-δ curves, F being the load applied on the reinforcement strip, and δ the relative displacement between reinforcement and substrate. In DL setups the determination of the force applied on one side of the specimens required the distribution of the load resultant (recorded by the load cell integrated in the testing machine) amongst the two reinforcement strips to be known. Despite the symmetry of the specimen and the set-up, most of the times strains and displacement were higher on the side where failure occurred, especially when DL1 was used. Despite the intrinsic variability of bond quality (due to a certain randomness of impregnation, especially with inorganic matrices) sSuch a non-uniform load distribution is likely to be related to the unavoidable small asymmetries, settlements and adjustments of the steel plates and of the bricks (which may not be perfectly aligned to each other) and, finally, to the friction between the reinforcement and the steel saddle. In order to estimate the distribution of the load on the two sides of the specimen, two strain gauges were placed on the free end of the textile (part of the textile extending from the end of the brick), providing a local measure of the load, given the Young's modulus of the fibres, which are assumed to behave as linear elastic. In order to ensure an accurate measurement of the strain and avoid the detachment of the strain gauge from the fibre, the free portion of the textile was impregnated with polymeric resin. The distribution of the total load (as recorded by the load cell) between the two reinforcement strips was taken to be proportional to the ratio of the two load values estimated by the readings of the strain gauges. By doing so, the load applied on each of the two reinforcement strips was determined and the F-δ curves were derived.

The ultimate loads of all bond tests carried out within the present experimental campaign are plotted in Fig. 14, having the anchorage length on the x-axis and the ultimate load divided by the width of the reinforcement strip on the y-axis, and collected in Table 6, with the aim of providing an overview of the ultimate load transferred by the tested reinforcement systems on the various considered

substrates. The debonding load generally increased for increasing anchorage length at least for short lengths. The effective anchorage length can be roughly estimated as between . Nevertheless, a lower increase resulted for anchorage lengths over 220 mm for SRG and 165 mm and 220 mm for CTRM, and between 220 mm and 440mm for SRG indicating that the effective anchorage length can be roughly estimated to be between these values. Analogously, the anchorage length for SRG resulted to be higher than 220 mm and lower than 440 mm. A more accurate estimate of the effective anchorage length is provided hereafter by means of the strain profiles will be discussed hereafter.

Table 6 Results of bond tests

Substrate	Fibre	Mortar	Setup	Anchorage Length [mm]	Width [mm]	Ultimate Load [kN]	Ultimate Load [kN/cm]	Failure mode	Institution
Brick	Carbon (3 layers)	Fibre-reinforced cement-based	DL1	55	404.0	3.42	0.86	c	UNIRM3
				55	404.0	3.01	0.75	b	
				220	404.0	4.18	1.05	a-c	
				220	404.0	5.29	1.32	a-c	
				220	404.0	6.11	1.53	a-c	
				220	404.0	5.01	1.25	a-c	
			DL2	55	404.0	3.88	0.97	c	
				55	404.0	4.26	1.07	c	
				110	404.0	5.02	1.26	c	
				110	404.0	4.61	1.15	c	
				165	404.0	5.19	1.30	c	
				165	404.0	5.70	1.42	a-c	
				220	404.0	6.59	1.65	a	
				220	404.0	5.83	1.46	b	
	Steel (1 layer)		DL2	55	404.0	4.87	1.22	a	
				55	404.0	4.08	1.02	a	
				55	404.0	3.63	0.91	a	
				220	404.0	7.61	1.90	b	
				220	404.0	6.76	1.69	b	
				220	404.0	6.27	1.57	b	
				220	404.0	6.37	1.59	b	
				220	404.0	6.36	1.59	b	
				220	404.0	6.46	1.62	b	
				440	404.0	7.78	1.94	b	
				440	404.0	7.03	1.76	a-b	
				440	404.0	7.59	1.90	b	
		Lime-based	SL	150	505.0	1.47	0.29	a	UMINHO
				150	505.0	1.62	0.32	a	
				150	505.0	1.23	0.25	a	
				150	505.0	1.58	0.32	b-c	
			SL sandblasted	150	505.0	2.97	0.59	b-c	
				150	505.0	2.30	0.46	b-c	
				150	505.0	2.87	0.57	b-c	
				150	505.0	3.70	0.74	b-c	
Stone	Basalt (2 layers)	Cement-based polymer modified	SL	85	10010.0	2.81	0.28	a	TECNALIA
				85	10010.0	3.16	0.31	a	
				85	10010.0	2.38	0.23	a	
				85	10010.0	1.84	0.18	a	
				85	10010.0	2.38	0.23	a	
				150	10010.0	3.08	0.30	c	
				150	10010.0	2.77	0.27	c	
				200	10010.0	3.69	0.36	c	
				200	10010.0	2.70	0.27	c	

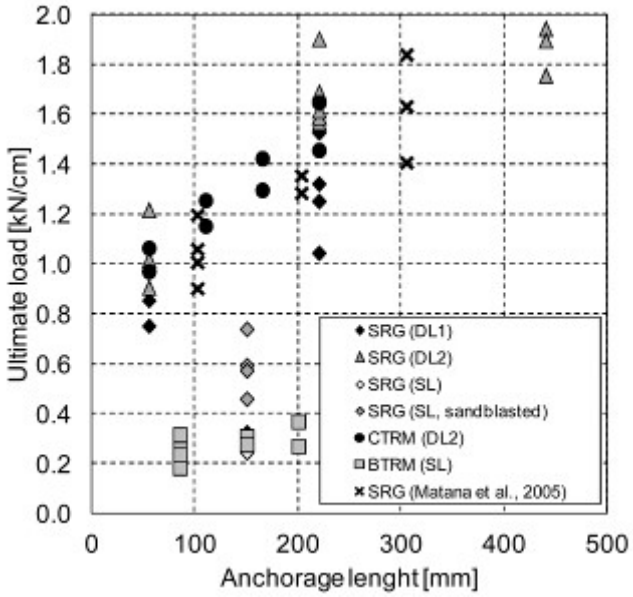

Fig. 14 Ultimate load vs. anchorage length

The lower strength displayed by the tests on SRG with 150 mm anchorage length is to be attributed to the lower resistance of the mortar, thus indicating the strong effect of the matrix on the debonding load. The comparison between tests on SRG carried out with the same mortar but different surface preparation procedures show the considerable effect of the mortar quality on the debonding load, which was in the order of 0.55 kN/cm for specimens with sandblasted surface, and ~~ca.~~about 0.3 kN/cm for untreated bricks.

The global F-δ curves are plotted in Figs. 15, 16, 17 for SGR, CTRM, and BTRM reinforcements, respectively (note that the load are divided by the reinforcement width): SRG reinforcement showed higher loads (15% on average) and stiffness values, with a brittle failure with maximum displacement in the order of 0.2-0.6 mm, while CTRM exhibited a longer horizontal branch up to displacement values generally larger than 1 mm, which is likely to be related to the slippage of the textile within the mortar matrix, as shown by the observed failure modes reported in Table 6. As shown in Table 5, bond tests on CTRM were carried out at UNIRM3 using both DL1 and DL2 setup schemes; although the choice of the setup configuration led to in-significant differences in the results, DL2 was found to be more reliable as it ensured that pure shear stresses were developed on the substrate-reinforcement interface and produced a better specimen symmetry. Load-displacement curves were unavailable by UMINHO due to unreliable LVDT readings. Finally, BTRM applied on stone substrate showed a much lower bond strength in the order of 0.2-0.4 kN/cm and resulted to be much more deformable, reaching displacements of about 2 mm.

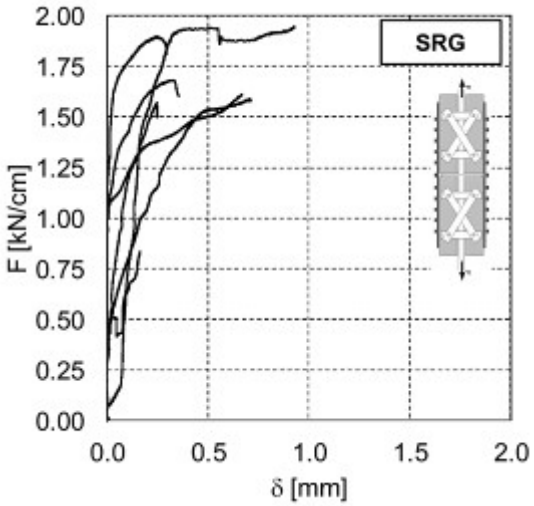

Fig. 15 Load-displacement curves for SRG reinforcement on brick substrates (only results of UNIRM3)

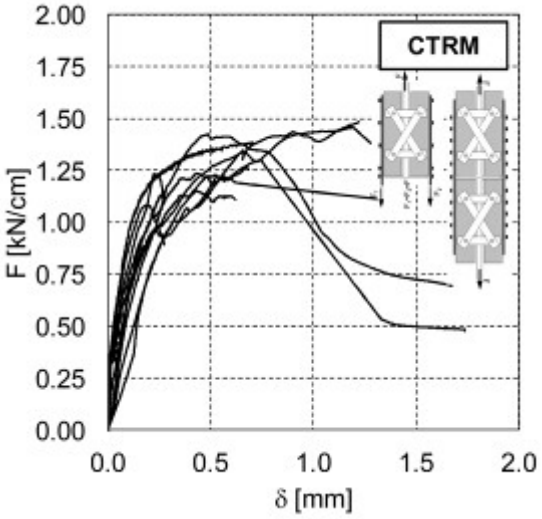

Fig. 16 Load-displacement curves for CTRM reinforcement on brick substrates

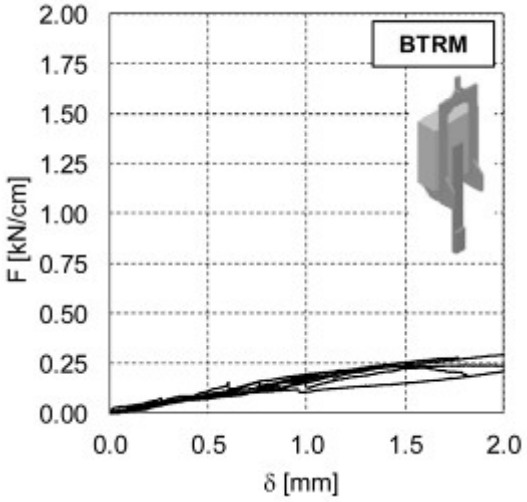

Fig. 17 Load-displacement curves for BTRM reinforcement on stone substrates

Data recorded by the strain gauges located on the reinforcement strips have been used to obtain strain profiles (i.e., strain vs. sensor position relation), as shown by Fig. 18 in which each curve refers to a different load level (F) ranging from 20% to 100% of the ultimate load (F_u). Recordings from strain gauges were considered reliable only until a crack propagated into the matrix disturbing the gauge reading. Under low force values, strains were detected only in the strain gauges placed in the vicinity to the loaded edge of the specimen and the higher was the applied load the larger was the length of the involved reinforcement strip, as it is shown by the strains measured by the gauges placed at further distance. As regards SRG, ~~until~~ as long as the load was below 40% of the maximum value the length of the reinforcement involved in the stress transmission was ca. 80mm and the strains were in the order of 1.5×10^{-3}. Then, as the load ~~grew~~increased, the strain of the fibres increased until a maximum value of ca. 3.5×10^{-3}. The length of reinforcement involved in the stress transmission was ca. 150 mm as revealed by the strain profiles of all the curves, with the exception of the last two lines (corresponding to F=80% F_u and F=F_u) in the bottom edge of the specimen, which may be related to an initial debonding of the reinforcement on this side.

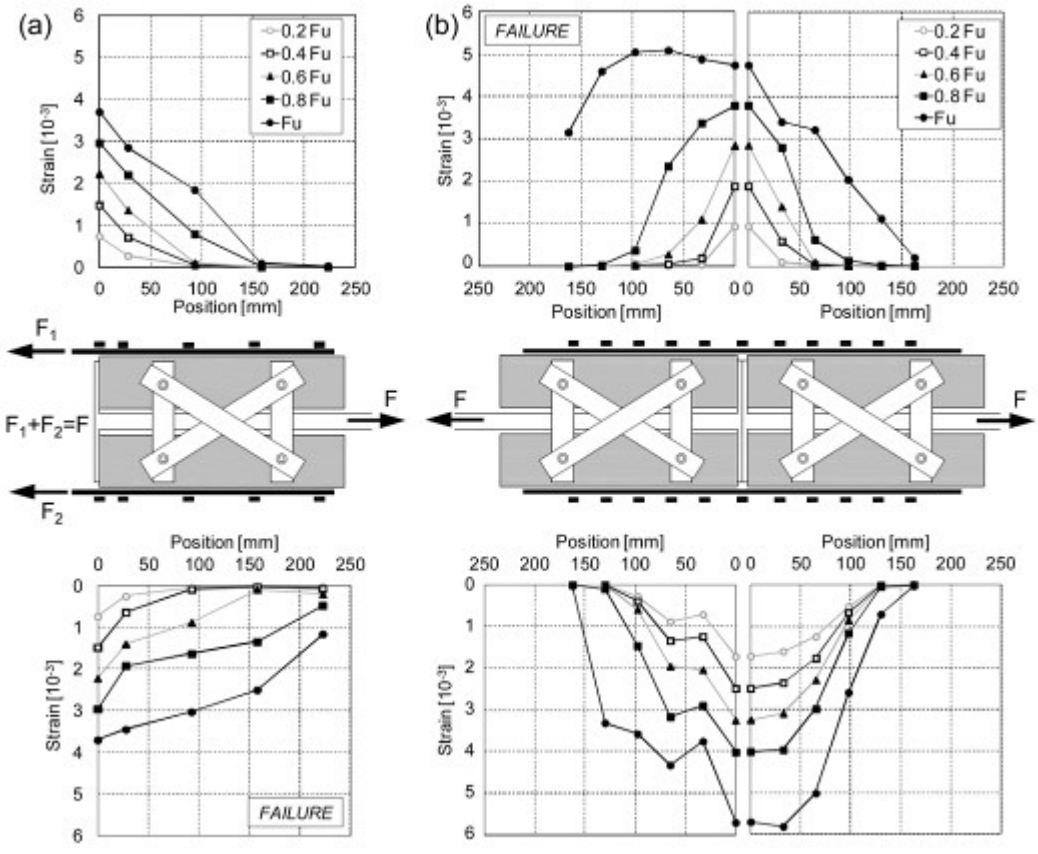

Fig. 18 Strain profiles for SRG (a) and CTRM (b) reinforcements

Concerning CTRM, the maximum strains where ~~ca.~~about 4×10^{-3} (at least ~~until~~ as long as the load was below 80% F_u) while the involved length was never higher than 150 mm with the exception of the last curves (corresponding to F=100% F_u)

whose shape indicated that debonding had already occurred, thus making the readings from strain gauges less reliable.

The shape of the strain profiles clearly displayed a variation in the concavity indicating the activation and subsequent development of debonding failure, especially on the edges of the specimens where it actually occurred. Once such a phenomenon was activated, the strain recorded by the gauges located in the vicinity of the specimen edge reached a maximum value (in the order of $3\text{-}4\times10^{-3}$ and $5\text{-}6\times10^{-3}$ for SRG and CTRM, respectively), which remained constant from that moment on.

On the base of the results of bond testing with different anchorage lengths and on the strain profiles derived from strain gauges, an effective anchorage length can be defined as that beyond which no increase of the load transferable through bond was observed. The extension of the anchored zone beyond the effective anchorage length does not provide any improvements in the maximum load. On the contrary, anchorage lengths lower than the effective one make the reinforcement unable to reach the maximum bonding load thus producing a debonding failure at lower load values. As regards SRG, the effective anchorage length was initially estimated to range between 220 mm and 440 mm; it can now be assumed to lie between 220 mm and 280 mm, at least based on the tests carried out at UNIRM3 with the same mortar and various anchorage lengths. The strain gauge placed at 220 mm distance from the specimen edge recorded non-null values only after the activation of debonding. Moreover, specimens tested with longer anchorage lengths (440 mm) were equipped with strain gauges at 280 mm distance and did not read any strains. Concerning CTRM, whose preliminary estimate was between 165 mm and 220 mm, the recording of the gauge at 162 mm which are null under a load of 80% of the maximum one suggested that the effective anchorage length can be assumed to be slightly higher than 165 mm.

Clearly, the values of debonding load and anchor length derived in the present study are only valid in case of pure shear while can't be considered reliable in case of bending (reinforcement of beams) or of curved surface of the substrate (reinforcement of arches and vaults), due to the presence of stresses normal to the substrate-reinforcement interface.

CONCLUSIONS

The mechanical performance of mortar-based reinforcement systems made out of steel, basalt, and carbon textiles has been investigated through an experimental campaign carried out by three laboratories, namely UNIRM3 (Italy), UMINHO (Portugal), and TECNALIA (Spain). Tests on tensile strength and bond capacity were carried out to provide some information on mechanical properties and testing methodologies of TRMs.

Within the present experimental campaign, steel reinforced grout (SRG) under tension displayed a much higher maximum stress (about 3000 N/mm^2) with respect to basalt textile reinforced mortar (BTRM) and carbon textile reinforced matrix (CTRM) which showed about 1200 N/mm^2 strength.

As for the Young's modulus, values in the order of 200 kN/mm^2 were found for SRG and CTRM, and 60 kN/mm^2 for BTRM. The stress-strain curves showed that, under tension, the mortar matrix is able to provide a significant contribution

to the composite's strength and stiffness only in the very first phase of the test (i.e., for low load values). After such an initial stage (uncracked specimen), a transition phase follows in which the mortar is cracked but is still able to provide a certain stiffening effect. Finally, in the last stage, the cracked mortar does not provide any contribution and the response is governed by the basically linear behaviour of the fibres up to a brittle failure. It was observed that the tensile strength of the composite is often smaller than that of the textile alone, which may be related to a non-uniform load distribution within the cords/yarns of the textile embedded in the mortar matrix (Hegger et al., 2006; Häußler-Combe and Hartig, 2007).

Different gripping methods were adopted in tensile tests. The use of aluminium tabs to clamp SRG specimens allowed for a good uniformity in the load transfer while in the case of BTRM and CTRM specimens, cracking occurred in the vicinity of the edge of the metal plates, which may be related to a certain stress concentration. A careful acquisition of strain and displacement is therefore needed so as to avoid the readings to be disturbed by the occurrence of cracks.

Bond tests were carried out on brick substrate with SRG and CTRM and on stone with BTRM, showing that higher bond performances are achieved with mortar matrices of higher strength, with stiffer textiles (the stiffer is the textile the longer is the transfer length, which usually leads to a higher bond performance), and with suitable substrate preparation techniques (e.g., sand-blasting) that increase the surface roughness. Strain profiles derived from strain gauge readings allowed the effective anchorage length to be estimated in the range of 220-280 mm for SRG and 165-220 mm for CTRM, for the tested TRM configurations.

Three main failure modes were identified: debonding at substrate-matrix interface and peeling off of the brick's surface (failure mode a), debonding at the textile-matrix interface (b) and slipping of the fibre rovings from the matrix (c). Failure mode (a) generally occurred for short bonded lengths with SRG reinforcements, while failure modes (b) and (c) were observed for long anchorage lengths and for CTRM and BTRM, due to the worse interlocking between textile and matrix. Even if carbon and basalt reinforcements are made out of bidirectional meshes, in which transverse fibre rovings improve the matrix-to-textile bond, telescopic sliding of the fibre roving was observed as a consequence of the smooth surface of the fabric and its bitumen coating. This phenomenon needs to be deeply investigated and its structural effects possibly exploited in those applications that prioritize fracture toughness over strength. A combined a-c failure mode occurred for CTRM specimens with intermediate anchorage length (probably close to the effective transfer length), including an initial partial debonding of the mortar until the development of a transversal crack and the subsequent slipping of the fibre from the matrix.

Based on the preliminary results of the present experimental campaign, failure in mortar-based composites may occur within the matrix, diversely from FRP-masonry assemblage where the substrate is generally the weakest element. Therefore, in order to prevent the textile to slide within the matrix, the fibre-to-mortar chemical bond and interlocking need to be improved. To this purpose, more textile layers with low fibre volume fractions provide better performances than single-layer high density textiles, allowing for more fibres to be in contact with the matrix and ensuring a higher shear strength at the textile-matrix interface.

The outcomes of the present work show that the behaviour of mortar based strengthening systems and their bond performance strongly depend on the

mechanical properties of matrix and textiles, on their volume ratios, on the layout of the textile, on the curing conditions, on the substrate mechanical properties and surface treatment. The present experimental study provides an overview on some relevant issues related to the response of mortar-based composites applied to masonry substrates, as well as on the testing methodologies. Nevertheless, a much larger quantity of experimental results are needed before some more general conclusions can be drawn and results can be directly applied in design practice.

REFERENCES

Aiello MA, Sciolti SM (2006) Bond analysis of masonry structures strengthened with CFRP sheets. Constr Build Mater 20:90-100

Ascione L, Feo L, Fraternali F (2005) Load carrying capacity of 2D FRP/strengthened masonry structures. Compos Part B-Eng 36(8):619-626

Balsamo A, Di Ludovico M, Prota A, Manfredi G (2011) Masonry walls strengthened with innovative composites. American Concr Inst, ACI Spec Publ 2(275):769-786

Borri A, Castori G, Corradi M (2011) Shear behavior of masonry panels strengthened by high strength steel cords. Constr Build Mater 25(2):494-503

Brameshuber W (2006) Textile reinforced concrete. State-of-the-art report of RILEM Technical Committee 201-TRC. Report 36, Bagneux, RILEM

Cancelli AN, Aiello MA, Casadei P (2007) Experimental investigation of bond properties of SRP/SRG - masonry systems. In: Fiber Reinforced Polymer Reinforcement for Concrete Structures - FRPRCS-8, Proc 8th Int Symp, Patras, Greece

Carbone I, de Felice G (2008) Bond performance of fibre reinforced grout on brickwork specimens. In: Proc SAHC 2008 6th International Conference on Structural Analysis of Historic Constructions, Bath, UK

Carbone I, de Felice G (2009) Debonding of CTRM composite on masonry support. In: Proc Prohitec 09 Int Conf on Protection of Historical Buildings, Rome, Italy

Carloni C, Subramaniam KV (2013) Investigation of sub-critical fatigue crack growth in FRP/concrete cohesive interface using digital image analysis. Compos Part B-Eng 51:35-43

Ceroni F, de Felice G, Grande E, Malena M, Mazzotti C, Sacco E, Valluzzi MR (2013). Modeling of the FRP-masonry bond behavior. THIS ISSUE.

CNR (2012). CNR-DT 200 R1/2012. Guide Lines for the Design and Construction of Externally Bonded FRP Systems for Strengthening Existing Structures. Italian Research Council, Italy.

Colombo I G, Magri A, Zani G, Colombo M, di Prisco M (2013) Textile Reinforced Concrete: experimental investigation on design parameters. RILEM Mater Struct. Doi: 10.1617/s11527-013-0017-5

Contamine R., Si Larbi A. Hamelin P. (2011) Contribution to direct tensile testing of textile reinforced concrete (TRC) composites. Mater Sci Eng, 528, pp. 8589–8598

Corradi M, Borri A, Vignoli A (2002) Strengthening techniques tested on masonry structures struck by the Umbria-Marche earthquake of 1997-1998. Constr Build Mater 16(4):229-239

Cuypers H, Wastiels J (2006) A stochastic cracking theory for the introduction of matrix multiple cracking in textile reinforced concrete under tensile loading. In: Proc 1st International RILEM Symposium. RILEM Technical Committee 201-TRC. Aachen, Germany, pp 193-202

D'Ambrisi A, Feo L, Focacci F (2013) Experimental and analytical investigation on bond between Carbon-FRCM materials and masonry. Compos Part B-Eng 46:15-20

EN 1015-11 (2007) Methods of test mortar for masonry - Part 11: Determination of flexural and compressive strength of hardened mortar

EN 1926 (2006) Natural stone test methods. Determination of uniaxial compressive strength

EN 772-1 (2002) Methods of test for masonry units - Part 1: Determination of compressive strength

Garmendia L, San-José JT, García D, Larrinaga P (2011) Rehabilitation of masonry arches with compatible advanced composite material. Constr Build Mater 25(12):4374-4385

Garmendia L, San-José JT, Larrinaga P, García D (2012) Textile Reinforced Mortar as strengthening material for masonry arches. Int J Architectural Heritage Doi:10.1080/15583058.2012.704480

Grande E, Imbimbo M, Sacco E (2011) Bond behaviour of CFRP laminates glued on clay bricks: Experimental and numerical study Part B-Eng 42(2):330-340

Grande E, Imbimbo M, Sacco E (2013) Modeling and numerical analysis of the bond behavior of masonry elements strengthened with SRP/SRG. Part B-Eng 55:128-138

Hartig J, Jesse F, Schicktanz K, Häußler-Combe U (2012) Influence of experimental setups on the apparent uniaxial tensile load-bearing capacity of Textile Reinforced Concrete specimens. RILEM Mater Struct 45(3):433-446

Häußler-Combe U, Hartig J (2007) Bond and failure mechanisms of textile reinforced concrete (TRC) under uniaxial tensile loading. Cem Concr Compos 29(4):279-289.

Hegger J, Will N, Bruckermann O, Voss S (2006) Load–bearing behaviour and simulation of textile reinforced concrete. RILEM Mater Struct 39(8):765-776

ICC (2013). AC434 Proposed acceptance criteria for masonry and concrete strengthening using fiber-reinforced cementitious matrix (FRCM) composite systems. ICC-Evaluation Service, Whittier, CA.

Malena M, de Felice G (2014) Externally bonded composites on a curved masonry substrate. Compos Struct (submitted)

Matana M, Nanni A, Dharani L, Silva P, Tunis G (2005) Bond performance of steel reinforced polymer and steel reinforced grout. In: Proc Int Symp on Bond Behaviour of FRP in Structures (BBFS), Hong Kong, China

Ohno S, Hannant DJ (1994) Modeling the stress–strain response of continuous fiber reinforced cement composites. ACI Mater J 91(3):306-312

Oliveira DV, Basilio I, Lourenço PB (2011) Experimental bond behavior of FRP sheets glued on brick masonry. ASCE J Compos Constr 15(1):32-41

Ortlepp R, Hampel U, Curbach M (2006) A new approach for evaluating bond capacity or TRC strengthening. Cem Concr Compos 28(7):589–597

Pacheco-Torgal F, Jalali S (2011) Cementitious building materials reinforced with vegetable fibres: A review. Constr Build Mater 25(2):575-581

Panizza M, Garbin E, Valluzzi MR, Modena C (2008) Bond behaviour of CFRP and GFRP laminates on brick masonry. In: Proc SAHC 2008 6th Int Conf on Structural Analysis of Historical Constructions, Bath, UK

Papanicolaou CG, Triantafillou TC, Karlos K, Papathanasiou M (2007) Textile-reinforced mortar (TRM) versus FRP as strengthening material of URM walls: in-plane cyclic loading. RILEM Mater Struct 40(10):1081-1097

Papanicolaou CG, Triantafillou TC, Papathanasiou M, Karlos K (2008) Textile-reinforced mortar (TRM) versus FRP as strengthening material of URM walls: out-of-plane cyclic loading. RILEM Mater Struct 41(1):143-157

Triantafillou TC, Fardis MN (1997) Strengthening of historic masonry structures with composite materials. RILEM Mater Struct 30:486-496

Valluzzi MR, Modena C, de Felice G (2014) Current practice and open issues in strengthening historical buildings with composites. THIS ISSUE.

Valluzzi MR, Oliveira DV, Caratelli A, Castori G, Corradi M, de Felice G, Garbin E, Garcia D, Garmendia L, Grande E, Ianniruberto U, Kwiecień A, Leone M, Lignola

GP, Lourenço PB, Malena M, Micelli F, Panizza M, Papanicolaou CG, Prota A, Sacco E, Triantafillou TC, Viskovic A, Zając B, Zuccarino G (2012) Round Robin test for composite-to-brick shear bond characterization. RILEM Mater Struct 45(12):1761-1791

Valluzzi MR, Valdemarca M, Modena C (2001) Behavior of brick masonry vaults strengthened by FRP laminates. ASCE J Compos Constr (5)3:163-169

LIST OF FIGURE CAPTIONS

LIST OF TABLE CAPTIONS

REVISED MANUSCRIPT
Version 01 | Date: 13.12.2013

MORTAR-BASED SYSTEMS FOR EXTERNALLY BONDED STRENGTHENING OF MASONRY

Gianmarco de Felice[1,*], Stefano De Santis[1], Leire Garmendia[2], Bahman Ghiassi[3], Pello Larrinaga[2], Paulo B. Lourenço[3], Daniel V. Oliveira[3], Catherine G. Papanicolaou[4]

[1] Department of Engineering, Roma Tre University, Rome, Italy
[2] Tecnalia Research & Innovation, Bilbao, Spain
[3] Department of Civil Engineering, ISISE, University of Minho, Guimaraes, Portugal
[4] Department of Civil Engineering, University of Patras, Patras, Greece

**** Corresponding author:***
E-mail: gianmarco.defelice@uniroma3.it
Telephone: +39.06.5733.6268
Fax: +39.06.5733.6265

ABSTRACT

Mortar-based composite materials appear particularly promising for use as externally bonded reinforcement systems for masonry structures. Nevertheless, their mechanical performance, which may significantly differ from that of fibre reinforced polymers (FRP), is still far from being fully investigated. Furthermore, standardized and reliable testing procedures have not been defined yet. The present paper provides an experimental campaign carried out by laboratories in Italy, Portugal and Spain. The performance of three reinforcement systems made out of steel, carbon and basalt textiles embedded in inorganic matrices has been investigated by means of uniaxial tensile coupon testing and bond tests on brick and stone substrates. The experimental results provide a contribution to the understanding of the structural behaviour of textile reinforced mortars against tension and shear bond stress, and to the definition of relevant test procedures.

Keywords: Masonry, Mortar-based composites, Textile reinforced mortar, Tensile tests, Bond tests.

1. INTRODUCTION

An increasing attention has been given in the recent years to the development of innovative technologies based on the use of composite materials for strengthening masonry structures by applying externally bonded reinforcement systems. Recent applications of fibre reinforced polymers (FRP) to vaults, columns and walls have demonstrated their effectiveness in increasing the load-carrying capacity and in upgrading the seismic strength (Triantafillou and Fardis,

1997; Valluzzi et al., 2001; Corradi et al., 2002; Ascione et al., 2005; Panizza et al., 2008; Grande et al., 2011; Oliveira et al., 2011; Valluzzi et al., 2014). Inorganic matrices may offer a lower bond strength with respect to FRPs, due to the possible occurrence of weaker failure modes within the reinforcement rather than within the substrate. However, they have some advantages in terms of overlay-to-substrate compatibility, transpirability, reversibility, fire resistance, cost, and applicability (Papanicolaou et al., 2007; 2008; Cancelli et al., 2007; Carbone and de Felice 2008; Borri et al., 2011; Garmendia et al., 2011; Malena and de Felice, 2014). Moreover, the use of textiles with inorganic matrix seems to be particularly appropriate for application to masonry structures, since the higher bond strength of polymeric matrix cannot be fully exploited because of the low intrinsic mechanical characteristics of the substrate (Aiello and Sciolti, 2006; Oliveira et al., 2011; Garmendia et al., 2012; Grande et al., 2013; Ceroni et al., 2014). Nevertheless, a deeper knowledge needs to be gained for designing mortar-based strengthening systems that are suitable for application to masonry substrates, as well as for identifying their mechanical properties (e.g., under direct tension or shear bond stress) through standardized testing methodologies.

Systemized research on similar systems, such as Textile Reinforced Concrete (TRC), has been conducted by the RILEM TC 201-TRC (Brameshuber, 2006) while ongoing research is currently undertaken by the follow-up TC 232-TDT (Test methods and design of textile reinforced concrete). Despite the fact that the main application target of TRC is integration in new civil structures rather than strengthening of existing ones, strong analogies exist between mortar-based reinforcement systems and TRC on numerous key issues, including testing methods (Contamine et al., 2011; Hartig et al., 2012), durability and mechanical behaviour. As for the case of tensile behaviour, numerous studies have been carried out (Hegger et al., 2006; Häußler-Combe and Hartig, 2007; Colombo et al., 2013). However, TRC matrices usually consist of high performance finely grained cement concrete, while lime-based mortars might be preferred when strengthening a masonry structure for moisture compatibility reasons and reversibility requirements. As for the reinforcement textiles, beyond those typically used in TRC (glass, carbon or aramid fibre bundles), steel cords (Borri et al., 2011), basalt (Balsamo et al., 2011), and natural fibres (Pacheco-Torgal and Jalali, 2011) may be potentially selected for the strengthening of masonry, provided that fabric layouts are designed to ensure adequate interlocking within a weaker matrix.

In the perspective of using textile reinforced mortar as strengthening system, more research is needed to explore the mortar-based composite-to-substrate bond performance, for which only few contributions have been provided to date, whose preliminary results suggest that significantly lower bond strength and different failure modes may be expected with respect to FRPs (see for instance: Ortlepp et al., 2006; Carbone and de Felice, 2009; D'Ambrisi et al., 2013, Carloni and Subramaniam, 2013).

The present work describes the results of an experimental campaign devoted to the investigation of the mechanical performance of reinforcement systems comprising fibrous textiles embedded in inorganic matrices. The research is currently on-going within the RILEM TC CSM (Composites for sustainable strengthening of masonry). Three research laboratories, affiliated with the University Roma Tre (Rome, Italy, UNIRM3), with the University of Minho (Guimarães, Portugal, UMINHO), and with Tecnalia Research & Innovation

(Bilbao, Spain, TECNALIA) were involved. The experimental programme comprised Steel Reinforced Grouts (SRG), Carbon Textile Reinforced Mortars (CTRM) and Basalt Textile Reinforced Mortars (BTRM). Both cement-based and lime-based mortars have been used as matrices. The three composite systems were characterised through direct unidirectional tensile tests. Then, the TRM-to-substrate bond performance was investigated using different test setups (single or double lap scheme) and considering various anchorage lengths, substrates (brick and stone), and surface preparation techniques. The work aims at providing a contribution to the understanding of the mechanics of TRM as reinforcing material and to the definition of test procedures drawing upon the experience gained from the involved research units.

2. MATERIALS

The properties of the materials used by the three laboratories involved in the experimental campaign are listed in Tables 1 and 2. The former includes the type, compressive strength (f_b, f_m) and the Young's modulus (E_b, E_m) of the substrates and mortar matrices (with subscripts 'b' and 'm' assigned to substrates and mortars, respectively). The tensile strength of the mortar matrices (f_m^t) is also reported. The latter contains the type, the wire properties (tensile strength, f_{fil}, Young's modulus, E_{fil}, and ultimate strain, $\varepsilon_{u,fil}$), textile properties (tensile resistance, f_t, Young's modulus, E_f, ultimate strain, ε_u and weight, W) and equivalent thickness of the textile (t) used for deriving the stress values. EN 1926 (2006), EN 772-1 (2002), and EN 1015-11 (2007) standards were followed for the tests on natural stones, bricks, and mortars, respectively.

Table 1 Compressive properties of substrates and matrices

Institution			Substrate			Matrix			
Name	Acronym	Country	Type	f_b N/mm^2	E_b N/mm^2	Type	f_m N/mm^2	E_m N/mm^2	f_m^t N/mm^2
Roma Tre University	UNIRM3	Italy	Brick	55.2	16000	Fibre-reinforced cement-based mortar	38.0	15000	7.5
University of Minho	UMINHO	Portugal	Brick	14.2	9500	Lime-based mortar	13.0	14000	
Tecnalia R&I	TECNALIA	Spain	Stone	21.0	5900	Cement-based polymer-modified mortar	22.6	15700	

Table 2 Textile tensile properties

Institution	Type	Filament (1)			Textile				
		f_{fil} N/mm^2	E_{fil} N/mm^2	$\varepsilon_{u,fil}$ %	f_t (2) N/mm^2	E_f (2) N/mm^2	ε_u (2) %	W (1) g/m^2	t (1) mm
UNIRM3	Steel	2474	207000	2.3	2396	192857	1.61	2110	0.256
	Carbon	4800	240000	1.8	1914	189361	1.18	168	0.047
UMINHO	Steel	3200	206000	–	3070	190000	1.6	1800	0.227
TECNALIA	Basalt	2100	89000	3.1	–	67000	–	235	0.035
	Steel	3200	206000	–	3070	190000	1.6	600	0.075

(1) Data provided by the manufacturers
(2) Data determined experimentally

The mortar used by UNIRM3 was based on a commercially available fibre-reinforced cementitious binder with pozzolanic additives, specifically designed for use in combination with fibre meshes for the reinforcement of masonry structures; the 28-days' compressive strength (derived from 50 mm cubic specimens) and the Young's modulus of the mortar was 38 N/mm^2 and 15000 N/mm^2, respectively. Solid clay bricks were used for bond testing, having a compressive strength of 55.2 N/mm^2 and a Young's modulus equal to 16000 N/mm^2 (derived from compression tests on 50 mm cubic samples). Both steel and carbon meshes were used; the former was a commercial tape-like product consisting of high carbon steel cords unidirectionally oriented (12 cords/inch, which is called by the producer 'medium density'), while the latter was a carbon fibre mesh (more specifically, a textile comprising carbon fibre rovings arranged in two orthogonal directions) made out of textile 4mm wide stripes placed 6mm apart.

Solid clay bricks with dimensions of 200×100×50 mm^3 were used as the substrate for the bond specimens prepared at UMINHO laboratory. The compressive strength of the bricks was characterized through compressive tests on six 40 mm cubic specimens, in the flatwise direction. A medium density steel mesh (12 cords/inch) was used as the reinforcement inserted in a pozzolanic lime-based mortar matrix (also based on an off-the-shelf dry mix) with 13 N/mm^2 compressive strength (much lower if compared to that used at UNIRM3, which contained cement) and 14000 N/mm^2 Young's modulus. The mortar was characterized by performing compressive tests on five cylindrical specimens with 50 mm diameter and 100 mm height at 28 days.

TECNALIA laboratory used basalt fibre and steel wire meshes. Basalt textile was a grid comprising bitumen-coated fibre rovings arranged along two orthogonal directions. The bitumen coating is typically used in order to enhance the mortar-to-textile bond and, hence, improve certain mechanical properties of the TRM. Basalt textile grid spacing was 20 mm × 20 mm, while steel wire fabric had a density of 4 cords/inch. A cementitious mortar was used as matrix containing less than 4% of organic resins. After a 28-day curing period, 40×40×160 mm^3 prisms were tested to determine the compressive strength and the Young's modulus of the mortar (22.6 N/mm^2 and 15700 N/mm^2, respectively). Stone units were used for bond testing, having 21 N/mm^2 compressive strength and 1300 N/mm^2 Young's modulus.

3. TENSILE TESTS

Despite the ultimate load may be sometimes difficult to be exploited, the tensile behaviour of EBRs may have a certain importance in some structural applications, such as shear reinforcement of masonry panels, extrados strengthening of arches and vaults, and confinement of columns. For this reason, direct tensile tests are required by standard codes (CNR, 2012; ICC, 2013) for the mechanical characterization of mortar-based reinforcement systems and are expected to become a fundamental step of the industrial process for product qualification purposes.

Direct tensile tests on the different TRM were carried out to in order derive the main mechanical properties of the strengthening systems, such as the tensile

strength and stiffness. An overview of the tests performed by the three laboratories involved in the research is shown in Table 3, in which the size of the specimens and the number of textile layers embedded in the mortar are also listed. UNIRM3 performed tests on CTRM and SRG plate specimens having an overall cross section area of 40 mm × 7 mm and a length of 800 mm and 700 mm, respectively. Tests were carried out after 28 days of curing by means of a universal MTS testing machine, equipped with a 500 kN hydraulic actuator, under displacement control at 0.005 mm/s rate (machine compliance < 0.05%). The applied load was measured by a load cell integrated in the testing machine, while the strains were recorded at 10 Hz frequency through four resistive strain gauges (having length of 10 mm and 0.07% precision). Strain gauges were positioned vertically, two per side and parallel to each other, and were applied directly on the fibres, embedded within the mortar layer. For SRG specimens, in order to ensure an accurate measurement of the strain and avoid the detachment of the strain gauge from the steel cords, a small portion of the textile was impregnated with polymeric resin. This was not necessary for CTRM specimens, as the strain gauge and the carbon yarn had approximately the same width (2 mm). The SRG specimens tested at UMINHO had 3 mm mortar cover in each side of the steel cords resulting in total specimen thickness of 6 mm. The specimens' width and length were equal to 50 mm and 450 mm, respectively. Monotonic tests were performed after 28 days of curing using a universal testing machine with a maximum load capacity of 200 kN, under displacement control at 0.033 mm/s constant rate. The applied load was recorded by a load cell integrated in the testing machine, while deformation was monitored by a clip gauge placed mid-height on the specimens. Finally, TECNALIA manufactured specimens with a 100 mm × 10 mm cross section area and 600 mm length. The ends of each specimen were reinforced with two additional layers of textile (extending 200 mm from end to mid-height), in order to promote the failure of the specimen in its middle third portion. Tests were performed on a 100 kN hydraulic testing machine, under displacement control and load measurement precision better than 0.3%. The deformation of the middle third portion was measured by means of two Linear Variable Differential Transformers (LVDT). All the experimental information obtained was recorded using a data logger at 5 Hz frequency.

In the following section on bond tests, it will be shown that in mortar-based EBRs the textile may slip within the matrix, especially when the bond with the mortar is weak (carbon and basalt fabrics in this case). In order to prevent premature debonding by slipping, more layers were placed in the reinforcement. Direct tensile tests have been carried out with the same number of layers used for bond tests.

Table 3 Overview of the direct tensile tests on strengthening systems

Institution	Basalt		Carbon	Steel		Specimen dimension [mm^3]
	2 layers	3 layers	3 layers	4 cords/inch	12 cords/inch	
UNIRM3			4			40×7×800
					4	40×7×700
UMINHO					4	50×6×450

TECNALIA	7	7		7		100×10×600

Based on the specific properties of the specimens tested and on available laboratory facilities, different solutions were developed by the three laboratories to ensure adequate clamping of the specimen, which is necessary to guarantee a uniform load transfer and avoid stress concentration in the gripping area (Fig. 1). UNIRM3 chose to leave each end of the specimen free of mortar and to apply aluminium tabs by means of a strong structural glue. Then, the tables were clamped within the wedges of the testing machine. A similar procedure was followed by UMINHO. Finally, TECNALIA gripped the ends of the TRM specimens by means of a mechanical device made out of two steel plates having rough surfaces (knurl); extra textile strip was placed between the steel plates and the specimen.

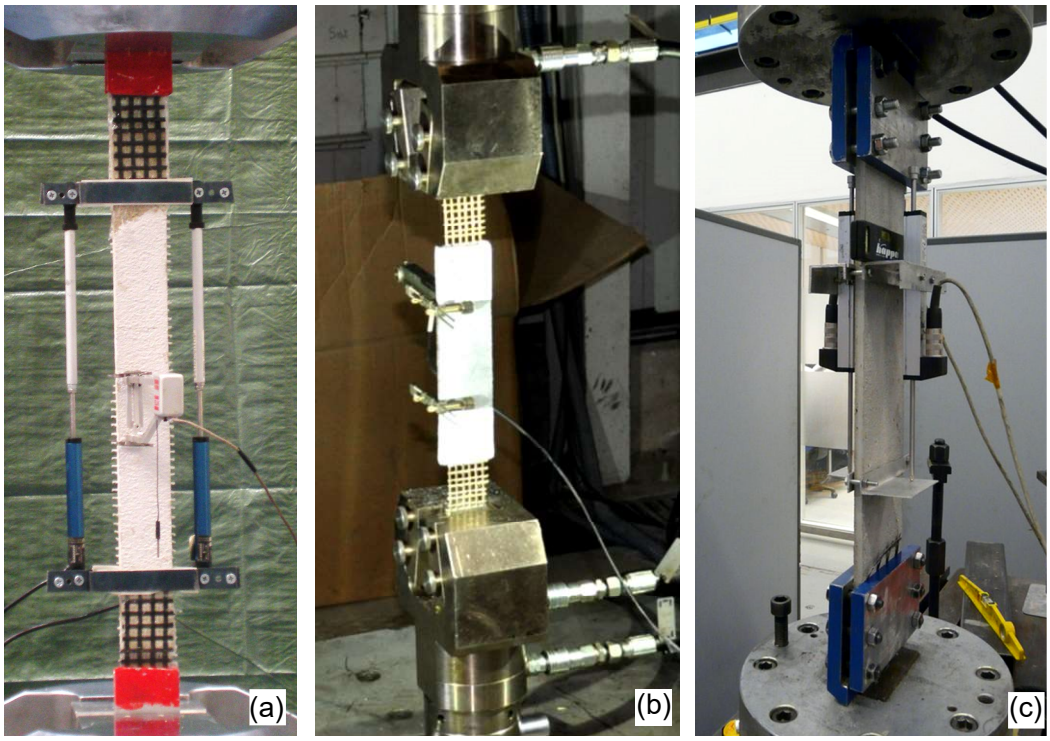

Fig. 1 Setup used for tensile tests by UNIRM3 (a), UMINHO (b) and TECNALIA (c)

The results of tensile tests are shown in Figs. 2, 3 and 4 for SRG, CTRM, and BTRM, respectively. Stress values correspond to the applied resultant load divided by the fibres' area. The latter is equal to the product of the number of layers, the specimen's width, and the textile design thickness in the direction of loading. The results (per TRM) present a relatively low scatter, especially for what concerns the maximum tensile stress (f_t), despite the differences in specimens' size and setups amongst different laboratories. Based on the present experimental investigation (in which slightly different setups have been used to test different composites under tension), higher strength values resulted from SRG specimens (in the order of 3000 N/mm^2), while BTRM and CTRM showed similar tensile resistance of about 1200 N/mm^2. The tensile strength of SRG specimens was found to be close to the tensile strength of the textile itself; for BTRM and CTRM specimens, though, a significant reduction was observed. The TRM with fibrous reinforcements (of more than one layers) may exhibit lower

tensile strength values than those of the textiles. Misalignment of the textile layers (or of the rovings of the same textile layer), areas in between layers not adequately filled with mortar, wear of fibres at the vicinity of crack edges and nonuniform stress distribution within the textile are some of the reasons why the tensile strength of the composite is generally less than that of the textile itself (Häußler-Combe and Hartig, 2007). Furthermore, according to the producers, this may be related to the mechanical stress induced on basalt and carbon wires in the textile manufacturing process.

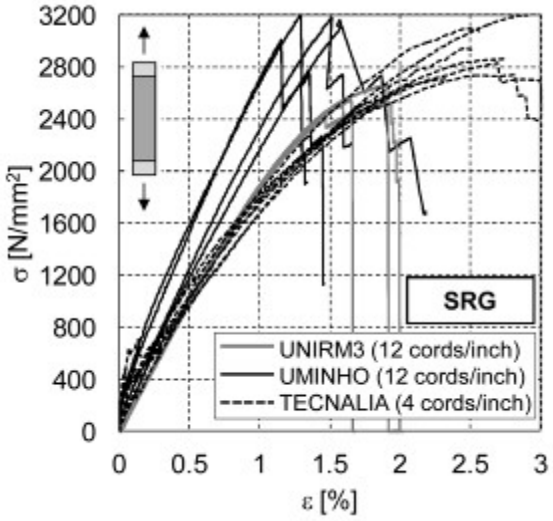

Fig. 2 Stress-strain curves of SRG specimens under uniaxial tension.

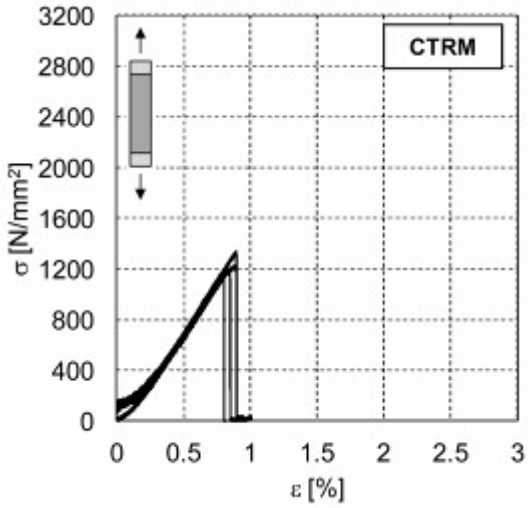

Fig. 3 Stress-strain curves of CTRM specimens under uniaxial tension.

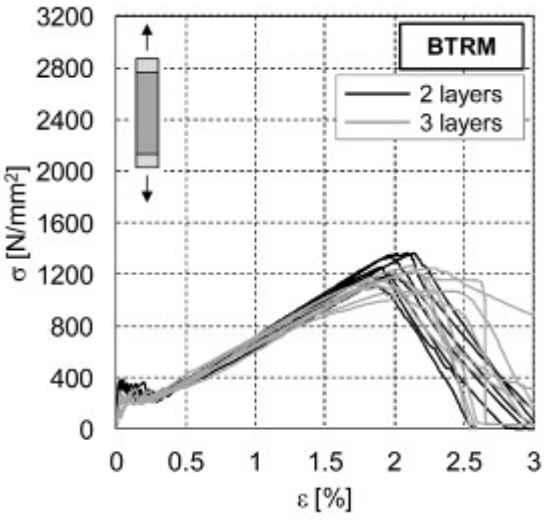

Fig. 4 Stress-strain curves of BTRM specimens under uniaxial tension.

In the present case, the tensile strength and stiffness of basalt TRM was not strongly influenced by the number of layers of textile embedded in the mortar, as shown in Fig. 4. The mechanical properties of mortar seems to affect only the initial non-cracked behaviour (which is clearly visible in Fig. 4 for BTRM specimens), while, once cracking occurs, a slight tension stiffening effect takes place without significant changes in the tensile strength of the composite. Conversely, the mortar plays a very important role in the bond mechanism as shown in the next section.

As for the ultimate strain (ε_u), i.e., the strain corresponding to the maximum stress, it was between 1% and 2% for SRG with higher density (12 cords/inch) and about 2.5-3% for SRG with lower density (4 cords/inch), about 0.8% for CTRM and, finally, about 2% for BTRM. The latter also showed a lower stiffness of about 6×10^4 N/mm^2, which is clearly related to the lower Young's modulus of the basalt filaments.

The three characteristic response stages of textile reinforced mortar (or concrete, as it is also termed) under uniaxial tensile loading (Brameshuber, 2006; Cuypers and Wastiels, 2006) are also observable on the stress-strain curves, especially for BTRM specimens. The first state corresponds to the behaviour of the uncracked specimen. When the tensile strength of the mortar is reached the first crack is formed and the second stage, the multiple cracking one, starts. The length of the multiple cracking stage was reduced with a higher number of reinforcement layers, as also observable in reinforced concrete (Cuypers and Wastiels, 2006). In the third stage (post-cracking stage during which the crack pattern has been stabilized), the composite is stressed up to the strength of the textile. The stiffness of the post-cracking stage was found to be lower than that of the textile if loaded independently; this is also reported by other studies (Brameshuber, 2006) and it is attributed to the premature failure of some filaments and to the premature debonding of either the core filaments (for textiles with uncoated rovings) (Ohno and Hannant, 1994) or the coated rovings. When the remaining filaments cannot bear the applied load, their fracture causes the whole composite to rupture. As shown in Figs. 2-4, failure of SRG specimens occurred as a progressive rupture of the cords, after a clear loss of linearity in the stress-strain response curve. CTRM specimens displayed a brittle failure of the

entire textile while in BTRM specimens some sort of progressive (although very fast) deterioration is visible in the post-peak branches of the stress-strain curves, which may be related to the textile unravelling within the matrix. The fundamental difference in the tensile behaviour of SRG with respect to CTRM and BTRM depends on the different structures of the reinforcement textiles. Steel cords are homogeneous and interact with the matrix at their perimeter, while carbon and basalt textiles are made out of bundles of filaments, such that only the external filaments directly interact with the mortar matrix, while the load transfer to the core ones relies on the bond between filaments. A bond failure between filaments within a bundle (telescopic rupture) may be responsible of larger displacements in CTRMs and BTRMs (Mobasher et al., 2006).

The results of all tensile tests are presented in Table 4, in which the elastic modulus (E_t) of the TRM specimens was obtained between stress values corresponding to 30% and 60% f_t, during the last stage (cracked specimen). At this stage, despite the matrix is cracked, the specimen is still working as a composite as the mortar between consecutive cracks provides both a stiffening effect and a load redistribution amongst the yarns/cords of the textile. At UNIRM3, in addition to global displacements, local strains were recorded by resistive strain gauges, placed directly on the textile (within the mortar), to avoid the influence of crack development on the acquired data and derive local measures in the middle portion of the specimen.

Table 4 Mean values of the results of tensile tests (standard deviation in brackets)

Reinforcement	Institution	f_t [N/mm^2]	E_t [N/mm^2]	ε_u [%]
SRG	UNIRM3	2558 (7.4%)	209805 (4.9%)	1.90 (13.2%)
	UMINHO	3134	217500	1.37
	TECNALIA	2959	150400	2.76
CTRM	UNIRM3	1191 (8.9%)	196525 (7.0%)	0.74 (9.5%)
BTRM (2 layers)	TECNALIA	1256	59000	1.96
BTRM (3 layers)	TECNALIA	1195	57000	2.10

Independently from the type of textile used, and from the mortar adopted as matrix, the crack development observed during tensile tests on TRM specimens was characterized by the presence of cracks transversal to the direction of the applied load, clearly identifiable in the response curves and visible during testing at low stress values. The crack spacing and width were dependent on the type and quantity of reinforcement and on the textile-to-matrix bond behaviour. Higher fibres' volume fractions, as well as fibres with higher stiffness, gave rise to denser crack patterns. A larger number of narrow cracks developed in SRG specimens, which may be related to a better interlocking between the steel cords (of uneven surface as they are made by twisting steel filaments) and the mortar. Improved bond conditions hinder slipping of the textile within the mortar and the development of few wide cracks. Transversal cracks sometimes developed in the vicinity of the aluminium tabs used to grip the samples (Fig. 5a), highlighting the importance of clamping in tensile testing. However, this was not evident for SRG specimens (Fig. 5b), probably due to the higher toughness of the material, and for BTRM specimens, where the end of the specimens were strengthened and cracks only appeared in their middle third (Fig. 6).

Fig. 5 Damage pattern in tensile tests: development of cracks in the vicinity of the aluminium plates in CTRM (a) and detachment of the mortar in SRG (b)

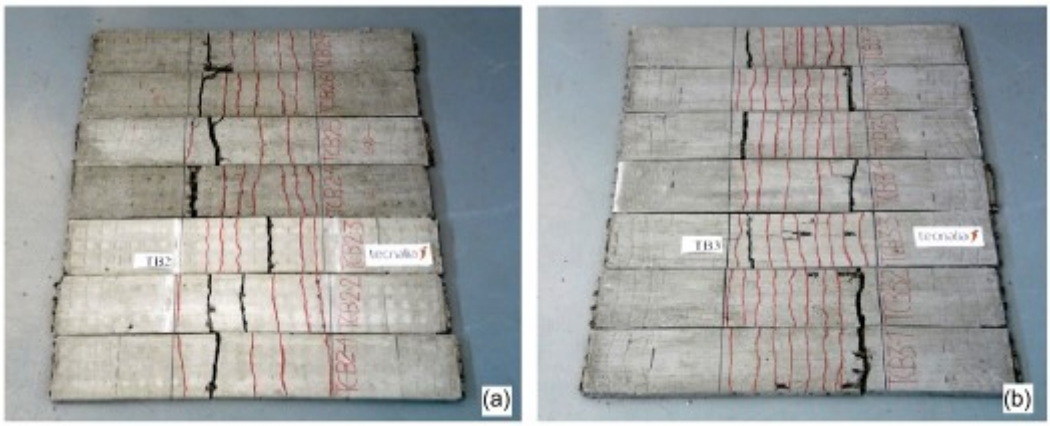

Fig. 6 Tensile tests on BTRM: development of the crack pattern in the middle third of the specimens on series TB2 with 2 layers (a) and TB3 with 3 layers (b)

4. BOND TESTS

4.1. Experimental programme and test setup

Tests on bond performance of TRM were carried out on brick and stone substrates. Brick units were tested by UNIRM3 and UMINHO with CTRM and SRG reinforcements, while stone units were used by TECNALIA to test BTRM reinforcements. An overview of the testing programme is given in Table 5. A standard wet lay-up procedure was followed to bond the steel, carbon or basalt textile sheets on either solid clay brick or stone substrates. The procedure involved the application of a 2-3 mm thick mortar layer on the block's surface (smoothing out any surface irregularities) and the subsequent bonding of the textile by hand and roller pressure. The textile was pressed slightly into the fresh mortar, which protruded through all the perforations between fibre rovings. The mortar was also applied in between layers (where applicable) and on top of the last textile

layer. The total thickness was 6-7 mm. The bond with the mortar matrix in carbon and basalt fabrics is weaker than in SRG, so premature slipping may occur. In order to prevent this kind of rupture, at least for short anchorage lengths, more layers of carbon and basalt were used. Curing of the TRM overlays was achieved in room conditions (about 15-20°C and 50-60% R.H.). More information regarding surface preparation techniques followed for specimens employing brick substrates will be given further on in the text. Table 5 Bond testing programme

	Fibre	Basalt (2 layers)	Carbon (3 layers)		Steel (1 layer)	
	Setup	SL	DL1	DL2	SL	DL2
	Brick		6	8		12
	Brick				8	
	Stone	9				

Aiming at avoiding the fibre rupture and focussing on bond performance, 2 layers of basalt and 3 layers of carbon were applied. As for steel, textiles made out of galvanized steel cords were used: one with 4 cords/inch (low density textile) and one with 12 cords/inch (medium density textile).

Drawing on previous experience on FRP (Valluzzi et al., 2012), four different shear bond testing setups were used: two single-lap (SL) and two double-lap (DL1 and DL2), as shown by Figs. 7 and 8. Very similar single-lap test schemes were used by UMINHO and TECNALIA, consisting of stiffened steel plates welded so as to form an angle of 90° (Fig. 7). At UMINHO, the specimens were supported appropriately to avoid misalignments in the load application and were loaded from above (Fig 7a). Tests were carried out under displacement control at a rate of 0.005 mm/s. The load was measured by a load cell while the slip between the reinforcement and the brick was measured by means of two LVDTs mounted at the loaded end. At TECNALIA, the specimens rested on the bottom of the steel frame and the reinforcement sheet was loaded from below (Fig 7b). Tests were performed using a 5 kN Lloys Universal Testing machine under displacement control at 0.008 mm/s rate. Displacements were measured by LVDTs located on both bonded and unbonded areas of the reinforcement.

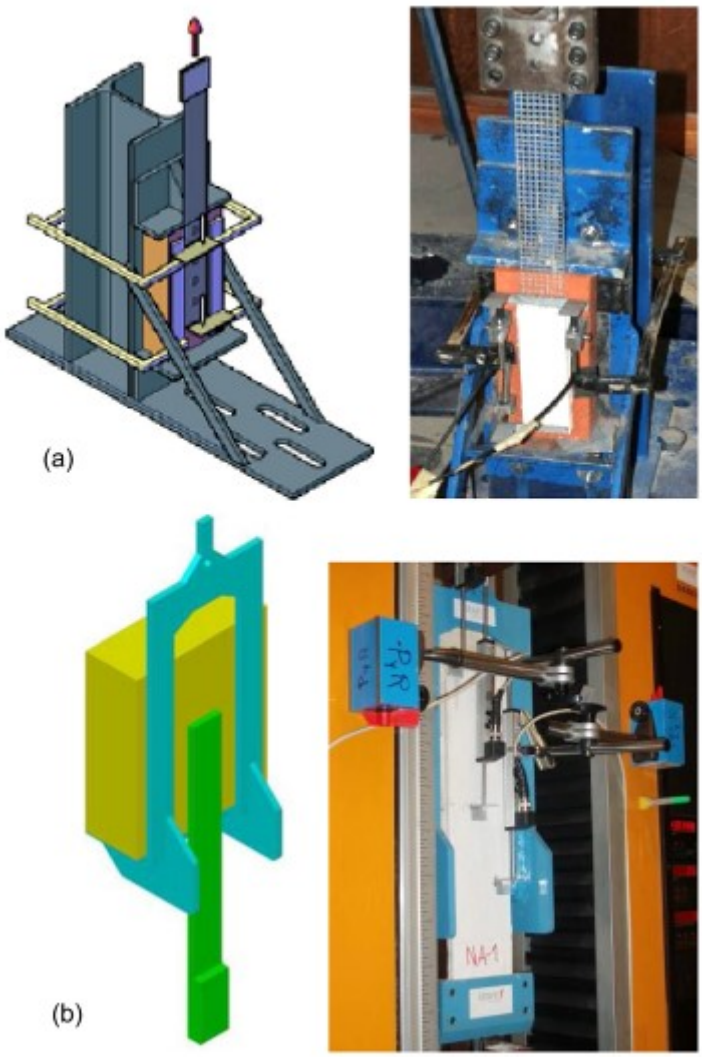

Fig. 7 Single-lap (SL) setup for bond shear tests carried out at UMINHO (a) and TECNALIA (b)

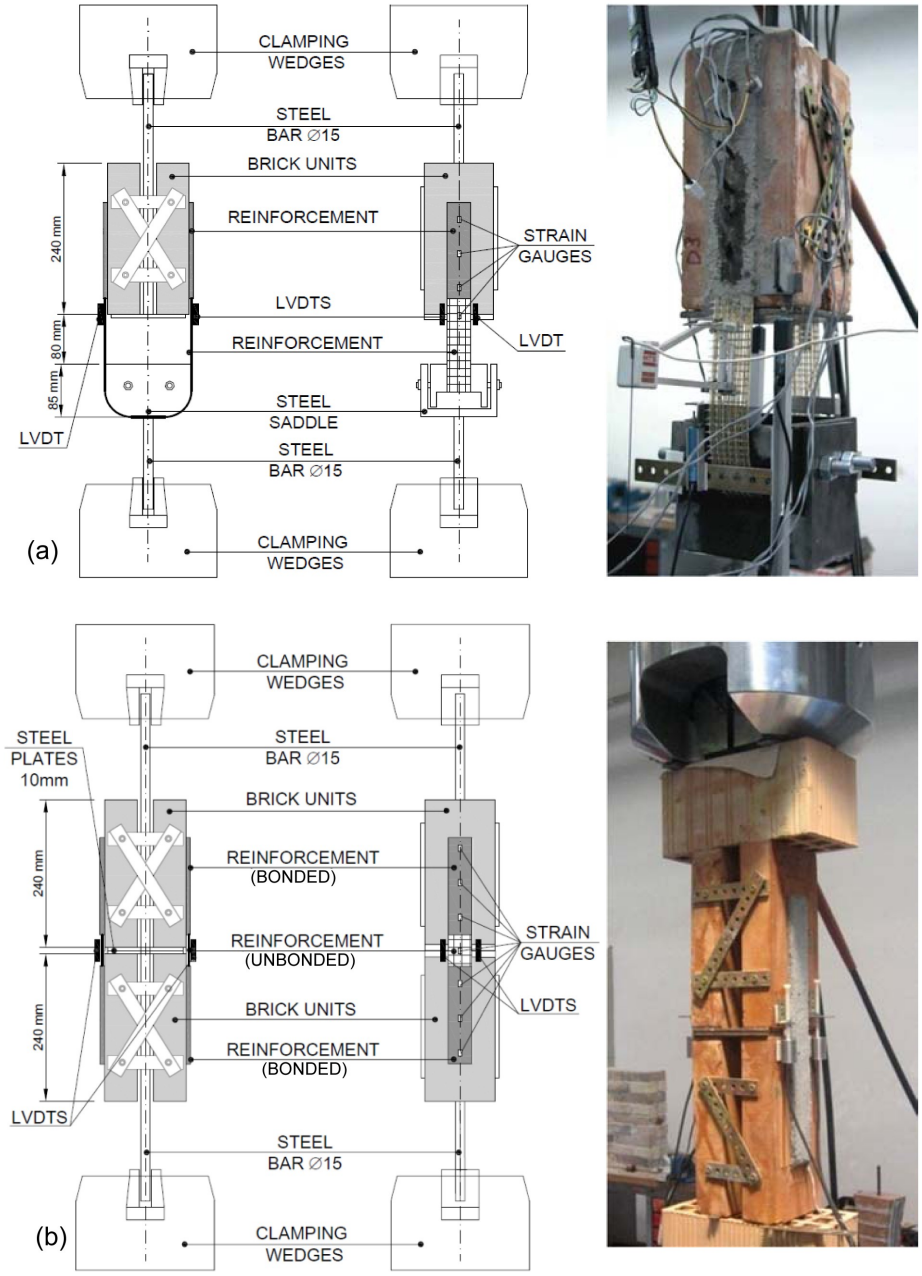

Fig. 8 Double lap setup for shear bond tests: type 1 (DL1, a) and type 2 (DL2, b)

UNIRM3 used double lap setups (DL). Specimens were built by joining together two bricks, placed parallel to each other at a pre-established distance, by means of steel plates; the reinforcement was then applied on both external faces. Setup DL1 (Fig. 8a) consisted of two or four bricks (depending on the anchorage length) pulled by the testing machine in one direction (upwards in the present case) through a steel bar welded to a steel plate (on which the bricks rested), while a continuous U-shaped reinforcement strip was pulled in the other direction (downwards) by means of a semi-circular steel saddle, having a diameter equal to the specimen width (1301 mm) so as to apply pure shear stresses on the brick-reinforcement interface. In test set-up DL2 (Fig. 8b) specimens were made out of four bricks. Two bricks were pulled upwards while the other two were pulled downwards by the testing machine. Two separate strengthening strips were applied on the external faces so as to connect two bricks by crossing the gap

between them. In UNIRM3 tests were performed by using a 500 kN MTS Universal Testing machine under displacement control at 0.005 mm/s rate. The load was recorded by a load cell integrated in the testing machine, while four LVDTs with 10mm stroke and 0.05 mm sensitivity were used to record relative displacements between reinforcement sheets and brick substrate. Finally, a set of 2.5 mm long strain gauges was also applied directly on the fibres (embedded in the matrix), with regular distance between each other, on both sides of the specimen to record local strain values along the reinforcement strip. Furthermore, a reinforcement band was left unbonded for a length of 10mm from the tip of the sample in order to avoid local stress concentrations induced by boundary effects.

Aiming at investigating the effect of the anchorage length on the ultimate load and at detecting information on the effective anchorage length (defined as that necessary for a complete stress transfer between reinforcement and substrate), various anchorage lengths were used, ranging from 55mm to 440 mm. More specifically, UNIRM3 tested the bond performance of SRG with 55 mm, 110 mm and 220 mm and CTRM with 55 mm, 220 mm and 440 mm for a total of 12 tests on SRG and 14 on CTRM; for these specimens bricks were used as a substrate. At UMINHO, a single anchorage length of 150 mm of SRG bonded on bricks was adopted with two different substrate preparation techniques; the first was minimal and involved cleaning and dusting the brick's surface while the second employed by sand-blasting. Finally, TECNALIA tested 9 stone specimens reinforced with BTRM with an anchorage length of 85 mm, 150 mm and 220 mm.

The experimental investigation made it possible to detect the TRM-to-substrate shear bond failure mode for the different textiles and anchorage lengths investigated as well as to derive the global response in terms of load vs. displacement relationships. Finally, the strain profile along the reinforcement strip, recorded for SRG specimens, gave some indication on the activation and propagation of the debonding phenomena and on the effective anchorage length.

4.2. Failure modes

Three failure modes were observed: debonding at substrate-matrix interface with peeling off of the brick surface (a), debonding at the textile-matrix interface (b) and slipping of the cords or rovings from the matrix (c), as sketched in Fig. 9. In the latter case the weak surface is the interface between the cords or rovings of the reinforcement textile and the mortar matrix they are embedded in.

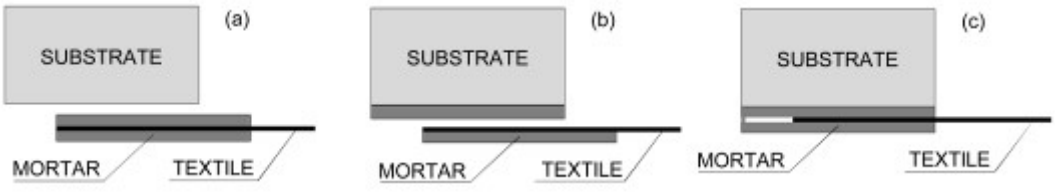

Fig. 9 Failure modes: debonding at substrate-matrix interface and peeling of the brick surface (a), debonding at fibre-matrix interface (b) and slipping of the textile from the matrix (c)

Differently from strengthening systems based on polymeric resins, mortar-based systems generally suffered a concentrated failure within the reinforcement layer, without extending the damage into the substrate. In SRG specimens the first failure mode (a) generally occurred with the shortest (55 mm) anchorage length

(Figs. 10a,b); this observation comes into agreement with the findings of previous experimental studies on concrete (Matana et al., 2005), thus indicating that shorter anchorage lengths may induce higher stresses in direction normal to the mortar-substrate interface, due to the misalignment between this surface and the textile embedded in the mortar matrix. These normal stresses are responsible of the extraction of aggregates from the grout (ripping) observed in the failure mode of specimens with shorter anchorage lengths. On the contrary, a brittle failure by debonding at the textile-matrix interface (b) was observed with the longest anchorage lengths (220 mm and 440 mm), as shown in Figs. 10c,d. Finally, it should be considered that different failure modes may be associated to different effective anchorage lengths as failure occurs on different surfaces. The effective length of failure mode (a) is likely to be shorter than that of mode (b). The results of the tests performed on SRG showed that the surface preparation may significantly affect the failure mode. In the brick specimens with minimal surface preparation, the mortar detached from the brick surface (failure mode a, Fig. 11a), while steel cord slipping with mortar cover separation was observed in the sand-blasted specimens, for both short and long anchorage lengths (combined failure mode b-c, Fig. 11b).

Similarly, debonding at the substrate-mortar interface was observed in stone specimens reinforced with BTRM with shorter anchorage lengths (85 mm), accompanied by the appearance of transversal cracks also in the unbounded portion of the reinforcement (Fig. 12a). On the contrary, the development of transversal cracks outside the bonded area occurred with the longest anchorage lengths (150 mm and 220 mm); the slipping of the fibres within the mortar matrix is clearly visible in Fig. 12b. As fibres and mortar matrix are subjected to the same elongation outside the bonded area due to equilibrium, such transversal cracks can only develop once the transfer of shear stresses between the substrate and the matrix and between matrix and fibres occurs, inducing the slipping of the textile within the mortar (failure mode c) to be activated before the other failure mechanisms.

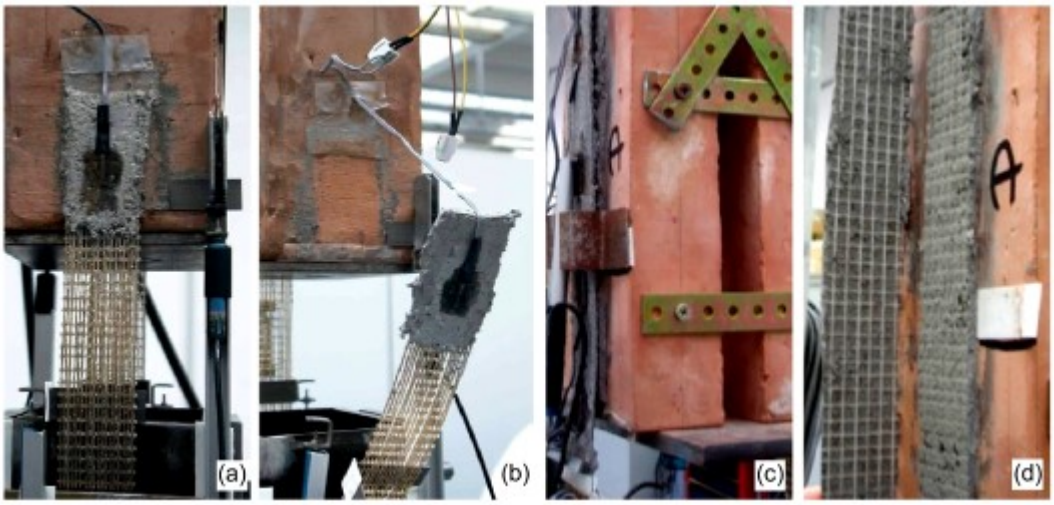

Fig. 10 Failure modes in SRG specimens with different anchorage lengths: debonding at substrate-matrix interface in specimens with anchorage length 55 mm (a, b) and at the textile-matrix interface in specimens with anchorage length 220 mm (c, d). (all specimens received the same minimal surface preparation prior to SRG application)

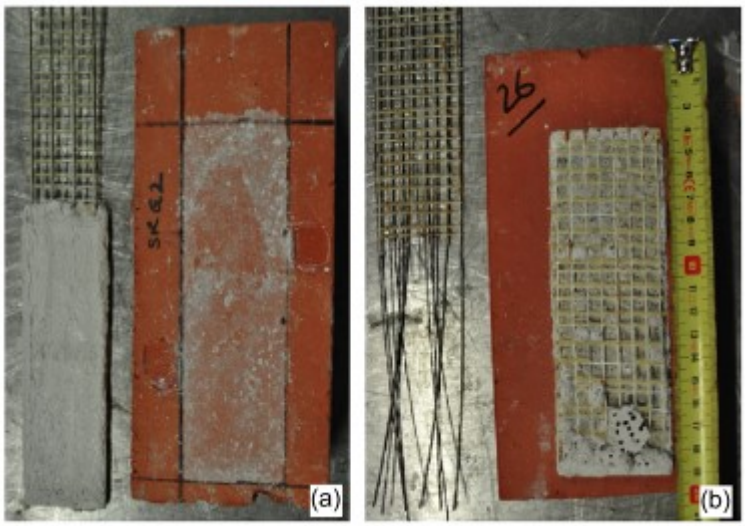

Fig. 11 Failure modes in SRG specimens with different surface preparations: specimens with minimal surface preparation (a) and specimens with sand-blasted surface (b)

Fig. 12 Failure modes in BTRM specimens: debonding at the substrate-matrix interface in specimens with anchorage length 85 mm (a) and slipping of the fibre rovings from the matrix in specimens with anchorage length 220 mm (b)

In CTRM specimens, the fibre-matrix interface generally resulted to be the weakest element; sliding of the fibre within the matrix (failure mode c) was observed in the specimens with the shortest anchorage lengths (55 mm and 110 mm), as shown by Figs. 13a,b while debonding at the fibre-matrix interface occurred for the longest one (220 mm), respectively. Intermediate anchorage lengths (165 mm) gave rise to a combined failure mode consisting in an initial partial debonding of the matrix until the development of a transversal crack, and in the subsequent sudden sliding of the fibre within the matrix inducing a brittle failure (Figs.13c,d).

The failure modes displayed by all the samples of the present experimental campaign are indicated in the next section.

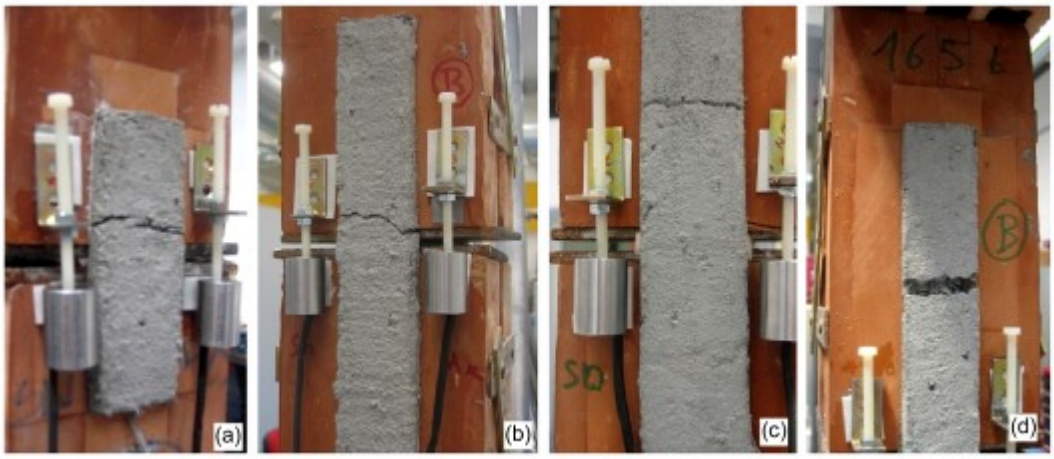

Fig. 13 Failure modes in CTRM specimens: slipping of the fibre rovings from the matrix in specimens with anchorage length 55 mm (a) and 110 mm (b) and combined failure with initial debonding of the matrix and subsequent slipping of the fibre rovings from the matrix in specimens with anchorage length 165 mm (c, d)

4.3. Results

The global response of the reinforcement-substrate systems under shear loads is represented by F-δ curves, F being the load applied on the reinforcement strip, and δ the relative displacement between reinforcement and substrate. In DL setups the determination of the force applied on one side of the specimens required the distribution of the load resultant (recorded by the load cell integrated in the testing machine) amongst the two reinforcement strips to be known. Despite the symmetry of the specimen and the set-up, most of the times strains and displacement were higher on the side where failure occurred, especially when DL1 was used. Despite the intrinsic variability of bond quality (due to a certain randomness of impregnation, especially with inorganic matrices) such a non-uniform load distribution is likely to be related to the unavoidable small asymmetries, settlements and adjustments of the steel plates and of the bricks (which may not be perfectly aligned to each other) and, finally, to the friction between the reinforcement and the steel saddle. In order to estimate the distribution of the load on the two sides of the specimen, two strain gauges were placed on the free end of the textile (part of the textile extending from the end of the brick), providing a local measure of the load, given the Young's modulus of the fibres, which are assumed to behave as linear elastic. In order to ensure an accurate measurement of the strain and avoid the detachment of the strain gauge from the fibre, the free portion of the textile was impregnated with polymeric resin. The distribution of the total load (as recorded by the load cell) between the two reinforcement strips was taken to be proportional to the ratio of the two load values estimated by the readings of the strain gauges. By doing so, the load applied on each of the two reinforcement strips was determined and the F-δ curves were derived.

The ultimate loads of all bond tests carried out within the present experimental campaign are plotted in Fig. 14, having the anchorage length on the x-axis and the ultimate load divided by the width of the reinforcement strip on the y-axis, and collected in Table 6, with the aim of providing an overview of the ultimate load transferred by the tested reinforcement systems on the various considered

substrates. The debonding load generally increased for increasing anchorage length at least for short lengths. The effective anchorage length can be roughly estimated as between 165 mm and 220 mm for CTRM, and between 220 mm and 440mm for SRG A more accurate estimate is provided hereafter by means of the strain profiles .

Table 6 Results of bond tests

Substrate	Fibre	Mortar	Setup	Anchorage Length [mm]	Width [mm]	Ultimate Load [kN]		Failure mode	
Brick	Carbon (3 layers)	Fibre-reinforced cement-based	DL1	55	40	3.42		c	
				55	40	3.01		b	
				220	40	4.18		a-c	
				220	40	5.29		a-c	
				220	40	6.11		a-c	
				220	40	5.01		a-c	
			DL2	55	40	3.88		c	
				55	40	4.26		c	
				110	40	5.02		c	
				110	40	4.61		c	
				165	40	5.19		c	
				165	40	5.70		a-c	
				220	40	6.59		a	
				220	40	5.83		b	
	Steel (1 layer)		DL2	55	40	4.87		a	
				55	40	4.08		a	
				55	40	3.63		a	
				220	40	7.61		b	
				220	40	6.76		b	
				220	40	6.27		b	
				220	40	6.37		b	
				220	40	6.36		b	
				220	40	6.46		b	
				440	40	7.78		b	
				440	40	7.03		a-b	
				440	40	7.59		b	
		Lime-based	SL	150	50	1.47		a	
				150	50	1.62		a	
				150	50	1.23		a	
				150	50	1.58		b-c	
			SL sandblasted	150	50	2.97		b-c	
				150	50	2.30		b-c	
				150	50	2.87		b-c	
				150	50	3.70		b-c	
Stone	Basalt (2 layers)	Cement-based polymer modified	SL	85	100	2.81		a	
				85	100	3.16		a	
				85	100	2.38		a	
				85	100	1.84		a	
				85	100	2.38		a	
				150	100	3.08		c	
				150	100	2.77		c	
				200	100	3.69		c	
				200	100	2.70		c	

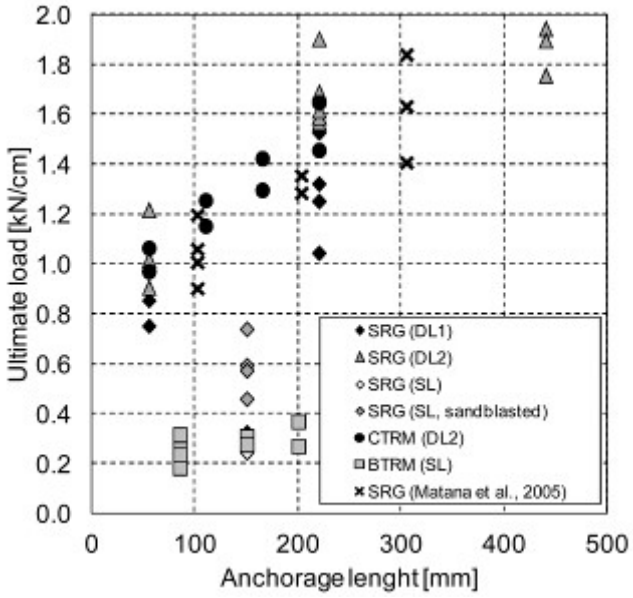

Fig. 14 Ultimate load vs. anchorage length

The lower strength displayed by the tests on SRG with 150 mm anchorage length is to be attributed to the lower resistance of the mortar, thus indicating the strong effect of the matrix on the debonding load. The comparison between tests on SRG carried out with the same mortar but different surface preparation procedures show the considerable effect of the mortar quality on the debonding load, which was in the order of 0.55 kN/cm for specimens with sandblasted surface, andabout 0.3 kN/cm for untreated bricks.

The global F-δ curves are plotted in Figs. 15, 16, 17 for SGR, CTRM, and BTRM reinforcements, respectively (note that the load are divided by the reinforcement width): SRG reinforcement showed higher loads (15% on average) and stiffness values, with a brittle failure with maximum displacement in the order of 0.2-0.6 mm, while CTRM exhibited a longer horizontal branch up to displacement values generally larger than 1 mm, which is likely to be related to the slippage of the textile within the mortar matrix, as shown by the observed failure modes reported in Table 6. As shown in Table 5, bond tests on CTRM were carried out at UNIRM3 using both DL1 and DL2 setup schemes; although the choice of the setup configuration led to insignificant differences in the results, DL2 was found to be more reliable as it ensured that pure shear stresses were developed on the substrate-reinforcement interface and produced a better specimen symmetry. Load-displacement curves were unavailable by UMINHO due to unreliable LVDT readings. Finally, BTRM applied on stone substrate showed a much lower bond strength in the order of 0.2-0.4 kN/cm and resulted to be much more deformable, reaching displacements of about 2 mm.

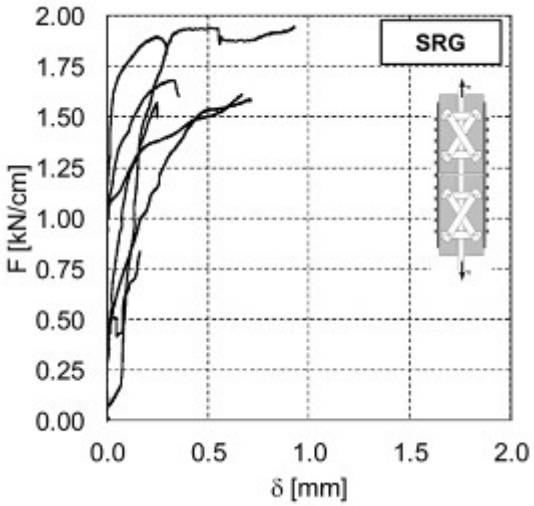

Fig. 15 Load-displacement curves for SRG reinforcement on brick substrates (only results of UNIRM3)

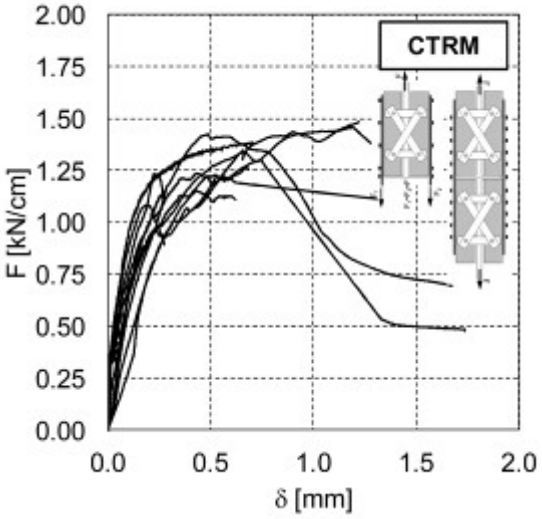

Fig. 16 Load-displacement curves for CTRM reinforcement on brick substrates

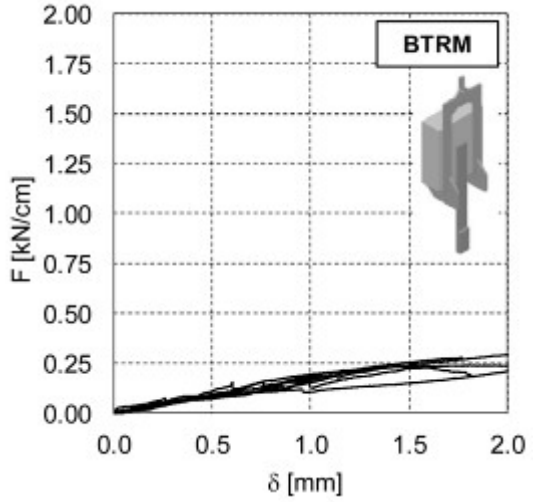

Fig. 17 Load-displacement curves for BTRM reinforcement on stone substrates

Data recorded by the strain gauges located on the reinforcement strips have been used to obtain strain profiles (i.e., strain vs. sensor position relation), as shown by Fig. 18 in which each curve refers to a different load level (F) ranging from 20% to 100% of the ultimate load (F_u). Recordings from strain gauges were considered reliable only until a crack propagated into the matrix disturbing the gauge reading. Under low force values, strains were detected only in the strain gauges placed in the vicinity to the loaded edge of the specimen and the higher was the applied load the larger was the length of the involved reinforcement strip, as it is shown by the strains measured by the gauges placed at further distance. As regards SRG, as long as the load was below 40% of the maximum value the length of the reinforcement involved in the stress transmission was ca. 80mm and the strains were in the order of 1.5×10^{-3}. Then, as the load increased, the strain of the fibres increased until a maximum value of ca. 3.5×10^{-3}. The length of reinforcement involved in the stress transmission was ca. 150 mm as revealed by the strain profiles of all the curves, with the exception of the last two lines (corresponding to F=80% F_u and F=F_u) in the bottom edge of the specimen, which may be related to an initial debonding of the reinforcement on this side.

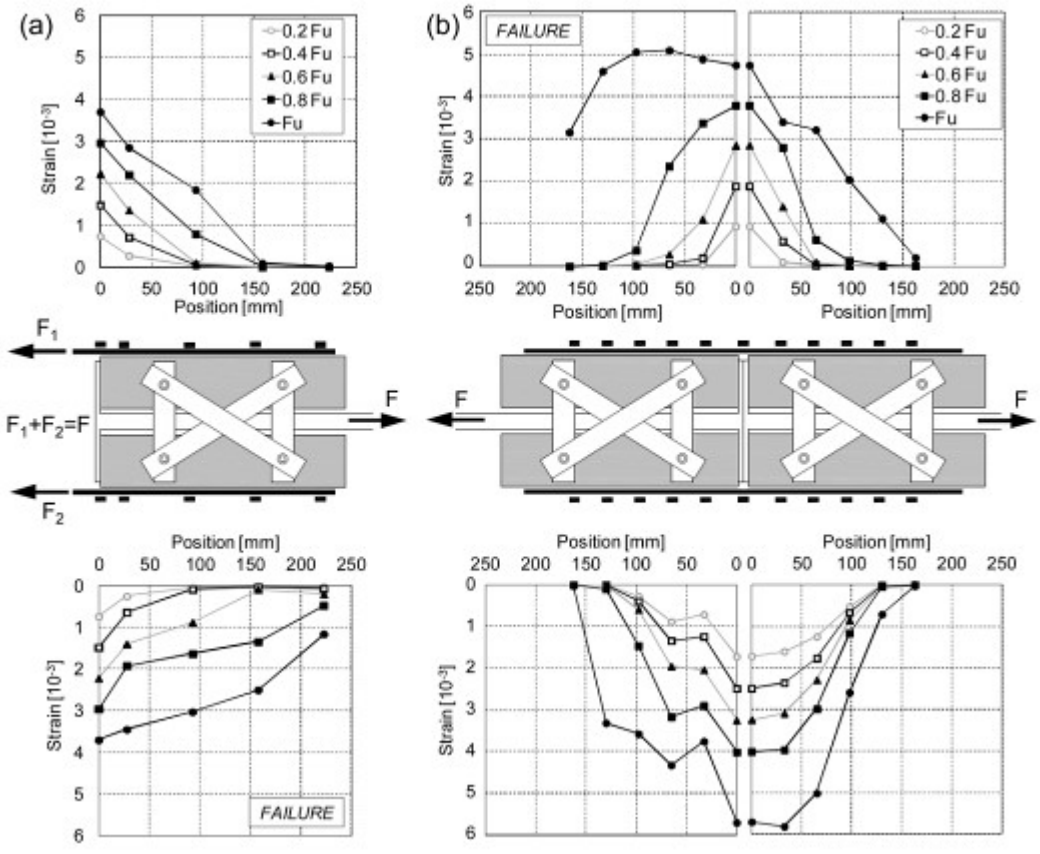

Fig. 18 Strain profiles for SRG (a) and CTRM (b) reinforcements

Concerning CTRM, the maximum strains whereabout 4×10^{-3} (at least as long as the load was below 80% F_u) while the involved length was never higher than 150 mm with the exception of the last curves (corresponding to F=100% F_u)

whose shape indicated that debonding had already occurred, thus making the readings from strain gauges less reliable.

The shape of the strain profiles clearly displayed a variation in the concavity indicating the activation and subsequent development of debonding failure, especially on the edges of the specimens where it actually occurred. Once such a phenomenon was activated, the strain recorded by the gauges located in the vicinity of the specimen edge reached a maximum value (in the order of $3\text{-}4\times10^{-3}$ and $5\text{-}6\times10^{-3}$ for SRG and CTRM, respectively), which remained constant from that moment on.

On the base of the results of bond testing with different anchorage lengths and on the strain profiles derived from strain gauges, an effective anchorage length can be defined as that beyond which no increase of the load transferable through bond was observed. The extension of the anchored zone beyond the effective anchorage length does not provide any improvements in the maximum load. On the contrary, anchorage lengths lower than the effective one make the reinforcement unable to reach the maximum bonding load thus producing a debonding failure at lower load values. As regards SRG, the effective anchorage length was initially estimated to range between 220 mm and 440 mm; it can now be assumed to lie between 220 mm and 280 mm, at least based on the tests carried out at UNIRM3 with the same mortar and various anchorage lengths. The strain gauge placed at 220 mm distance from the specimen edge recorded non-null values only after the activation of debonding. Moreover, specimens tested with longer anchorage lengths (440 mm) were equipped with strain gauges at 280 mm distance and did not read any strains. Concerning CTRM, whose preliminary estimate was between 165 mm and 220 mm, the recording of the gauge at 162 mm which are null under a load of 80% of the maximum one suggested that the effective anchorage length can be assumed to be slightly higher than 165 mm.

Clearly, the values of debonding load and anchor length derived in the present study are only valid in case of pure shear while can't be considered reliable in case of bending (reinforcement of beams) or of curved surface of the substrate (reinforcement of arches and vaults), due to the presence of stresses normal to the substrate-reinforcement interface.

CONCLUSIONS

The mechanical performance of mortar-based reinforcement systems made out of steel, basalt, and carbon textiles has been investigated through an experimental campaign carried out by three laboratories, namely UNIRM3 (Italy), UMINHO (Portugal), and TECNALIA (Spain). Tests on tensile strength and bond capacity were carried out to provide some information on mechanical properties and testing methodologies of TRMs.

Within the present experimental campaign, steel reinforced grout (SRG) under tension displayed a much higher maximum stress (about 3000 N/mm^2) with respect to basalt textile reinforced mortar (BTRM) and carbon textile reinforced matrix (CTRM) which showed about 1200 N/mm^2 strength.

As for the Young's modulus, values in the order of 200 kN/mm^2 were found for SRG and CTRM, and 60 kN/mm^2 for BTRM. The stress-strain curves showed that, under tension, the mortar matrix is able to provide a significant contribution

to the composite's strength and stiffness only in the very first phase of the test (i.e., for low load values). After such an initial stage (uncracked specimen), a transition phase follows in which the mortar is cracked but is still able to provide a certain stiffening effect. Finally, in the last stage, the cracked mortar does not provide any contribution and the response is governed by the basically linear behaviour of the fibres up to a brittle failure. It was observed that the tensile strength of the composite is often smaller than that of the textile alone, which may be related to a non-uniform load distribution within the cords/yarns of the textile embedded in the mortar matrix (Hegger et al., 2006; Häußler-Combe and Hartig, 2007).

Different gripping methods were adopted in tensile tests. The use of aluminium tabs to clamp SRG specimens allowed for a good uniformity in the load transfer while in the case of BTRM and CTRM specimens, cracking occurred in the vicinity of the edge of the metal plates, which may be related to a certain stress concentration. A careful acquisition of strain and displacement is therefore needed so as to avoid the readings to be disturbed by the occurrence of cracks.

Bond tests were carried out on brick substrate with SRG and CTRM and on stone with BTRM, showing that higher bond performances are achieved with mortar matrices of higher strength, with stiffer textiles (the stiffer is the textile the longer is the transfer length, which usually leads to a higher bond performance), and with suitable substrate preparation techniques (e.g., sand-blasting) that increase the surface roughness. Strain profiles derived from strain gauge readings allowed the effective anchorage length to be estimated in the range of 220-280 mm for SRG and 165-220 mm for CTRM, for the tested TRM configurations.

Three main failure modes were identified: debonding at substrate-matrix interface and peeling off of the brick's surface (failure mode a), debonding at the textile-matrix interface (b) and slipping of the fibre rovings from the matrix (c). Failure mode (a) generally occurred for short bonded lengths with SRG reinforcements, while failure modes (b) and (c) were observed for long anchorage lengths and for CTRM and BTRM, due to the worse interlocking between textile and matrix. Even if carbon and basalt reinforcements are made out of bidirectional meshes, in which transverse fibre rovings improve the matrix-to-textile bond, telescopic sliding of the fibre roving was observed as a consequence of the smooth surface of the fabric and its bitumen coating. This phenomenon needs to be deeply investigated and its structural effects possibly exploited in those applications that prioritize fracture toughness over strength. A combined a-c failure mode occurred for CTRM specimens with intermediate anchorage length (probably close to the effective transfer length), including an initial partial debonding of the mortar until the development of a transversal crack and the subsequent slipping of the fibre from the matrix.

Based on the preliminary results of the present experimental campaign, failure in mortar-based composites may occur within the matrix, diversely from FRP-masonry assemblage where the substrate is generally the weakest element. Therefore, in order to prevent the textile to slide within the matrix, the fibre-to-mortar chemical bond and interlocking need to be improved. To this purpose, more textile layers with low fibre volume fractions provide better performances than single-layer high density textiles, allowing for more fibres to be in contact with the matrix and ensuring a higher shear strength at the textile-matrix interface.

The outcomes of the present work show that the behaviour of mortar based strengthening systems and their bond performance strongly depend on the

mechanical properties of matrix and textiles, on their volume ratios, on the layout of the textile, on the curing conditions, on the substrate mechanical properties and surface treatment. The present experimental study provides an overview on some relevant issues related to the response of mortar-based composites applied to masonry substrates, as well as on the testing methodologies. Nevertheless, a much larger quantity of experimental results are needed before some more general conclusions can be drawn and results can be directly applied in design practice.

REFERENCES

Aiello MA, Sciolti SM (2006) Bond analysis of masonry structures strengthened with CFRP sheets. Constr Build Mater 20:90-100

Ascione L, Feo L, Fraternali F (2005) Load carrying capacity of 2D FRP/strengthened masonry structures. Compos Part B-Eng 36(8):619-626

Balsamo A, Di Ludovico M, Prota A, Manfredi G (2011) Masonry walls strengthened with innovative composites. American Concr Inst, ACI Spec Publ 2(275):769-786

Borri A, Castori G, Corradi M (2011) Shear behavior of masonry panels strengthened by high strength steel cords. Constr Build Mater 25(2):494-503

Brameshuber W (2006) Textile reinforced concrete. State-of-the-art report of RILEM Technical Committee 201-TRC. Report 36, Bagneux, RILEM

Cancelli AN, Aiello MA, Casadei P (2007) Experimental investigation of bond properties of SRP/SRG - masonry systems. In: Fiber Reinforced Polymer Reinforcement for Concrete Structures - FRPRCS-8, Proc 8th Int Symp, Patras, Greece

Carbone I, de Felice G (2008) Bond performance of fibre reinforced grout on brickwork specimens. In: Proc SAHC 2008 6th International Conference on Structural Analysis of Historic Constructions, Bath, UK

Carbone I, de Felice G (2009) Debonding of CTRM composite on masonry support. In: Proc Prohitec 09 Int Conf on Protection of Historical Buildings, Rome, Italy

Carloni C, Subramaniam KV (2013) Investigation of sub-critical fatigue crack growth in FRP/concrete cohesive interface using digital image analysis. Compos Part B-Eng 51:35-43

Ceroni F, de Felice G, Grande E, Malena M, Mazzotti C, Sacco E, Valluzzi MR (2013). Modeling of the FRP-masonry bond behavior. THIS ISSUE.

CNR (2012). CNR-DT 200 R1/2012. Guide Lines for the Design and Construction of Externally Bonded FRP Systems for Strengthening Existing Structures. Italian Research Council, Italy.Colombo I G, Magri A, Zani G, Colombo M, di Prisco M (2013) Textile Reinforced Concrete: experimental investigation on design parameters. RILEM Mater Struct. Doi: 10.1617/s11527-013-0017-5

Contamine R., Si Larbi A. Hamelin P. (2011) Contribution to direct tensile testing of textile reinforced concrete (TRC) composites. Mater Sci Eng, 528, pp. 8589–8598

Corradi M, Borri A, Vignoli A (2002) Strengthening techniques tested on masonry structures struck by the Umbria-Marche earthquake of 1997-1998. Constr Build Mater 16(4):229-239

Cuypers H, Wastiels J (2006) A stochastic cracking theory for the introduction of matrix multiple cracking in textile reinforced concrete under tensile loading. In: Proc 1st International RILEM Symposium. RILEM Technical Committee 201-TRC. Aachen, Germany, pp 193-202

D'Ambrisi A, Feo L, Focacci F (2013) Experimental and analytical investigation on bond between Carbon-FRCM materials and masonry. Compos Part B-Eng 46:15-20

EN 1015-11 (2007) Methods of test mortar for masonry - Part 11: Determination of flexural and compressive strength of hardened mortar

EN 1926 (2006) Natural stone test methods. Determination of uniaxial compressive strengthEN 772-1 (2002) Methods of test for masonry units - Part 1: Determination of compressive strength

Garmendia L, San-José JT, García D, Larrinaga P (2011) Rehabilitation of masonry arches with compatible advanced composite material. Constr Build Mater 25(12):4374-4385

Garmendia L, San-José JT, Larrinaga P, García D (2012) Textile Reinforced Mortar as strengthening material for masonry arches. Int J Architectural Heritage Doi:10.1080/15583058.2012.704480

Grande E, Imbimbo M, Sacco E (2011) Bond behaviour of CFRP laminates glued on clay bricks: Experimental and numerical study Part B-Eng 42(2):330-340

Grande E, Imbimbo M, Sacco E (2013) Modeling and numerical analysis of the bond behavior of masonry elements strengthened with SRP/SRG. Part B-Eng 55:128-138

Hartig J, Jesse F, Schicktanz K, Häußler-Combe U (2012) Influence of experimental setups on the apparent uniaxial tensile load-bearing capacity of Textile Reinforced Concrete specimens. RILEM Mater Struct 45(3):433-446

Häußler-Combe U, Hartig J (2007) Bond and failure mechanisms of textile reinforced concrete (TRC) under uniaxial tensile loading. Cem Concr Compos 29(4):279-289.

Hegger J, Will N, Bruckermann O, Voss S (2006) Load–bearing behaviour and simulation of textile reinforced concrete. RILEM Mater Struct 39(8):765-776

ICC (2013). AC434 Proposed acceptance criteria for masonry and concrete strengthening using fiber-reinforced cementitious matrix (FRCM) composite systems. ICC-Evaluation Service, Whittier, CA.Malena M, de Felice G (2014) Externally bonded composites on a curved masonry substrate. Compos Struct (submitted)

Matana M, Nanni A, Dharani L, Silva P, Tunis G (2005) Bond performance of steel reinforced polymer and steel reinforced grout. In: Proc Int Symp on Bond Behaviour of FRP in Structures (BBFS), Hong Kong, China

Ohno S, Hannant DJ (1994) Modeling the stress–strain response of continuous fiber reinforced cement composites. ACI Mater J 91(3):306-312

Oliveira DV, Basilio I, Lourenço PB (2011) Experimental bond behavior of FRP sheets glued on brick masonry. ASCE J Compos Constr 15(1):32-41

Ortlepp R, Hampel U, Curbach M (2006) A new approach for evaluating bond capacity or TRC strengthening. Cem Concr Compos 28(7):589–597

Pacheco-Torgal F, Jalali S (2011) Cementitious building materials reinforced with vegetable fibres: A review. Constr Build Mater 25(2):575-581

Panizza M, Garbin E, Valluzzi MR, Modena C (2008) Bond behaviour of CFRP and GFRP laminates on brick masonry. In: Proc SAHC 2008 6th Int Conf on Structural Analysis of Historical Constructions, Bath, UK

Papanicolaou CG, Triantafillou TC, Karlos K, Papathanasiou M (2007) Textile-reinforced mortar (TRM) versus FRP as strengthening material of URM walls: in-plane cyclic loading. RILEM Mater Struct 40(10):1081-1097

Papanicolaou CG, Triantafillou TC, Papathanasiou M, Karlos K (2008) Textile-reinforced mortar (TRM) versus FRP as strengthening material of URM walls: out-of-plane cyclic loading. RILEM Mater Struct 41(1):143-157

Triantafillou TC, Fardis MN (1997) Strengthening of historic masonry structures with composite materials. RILEM Mater Struct 30:486-496

Valluzzi MR, Modena C, de Felice G (2014) Current practice and open issues in strengthening historical buildings with composites. THIS ISSUE.

Valluzzi MR, Oliveira DV, Caratelli A, Castori G, Corradi M, de Felice G, Garbin E, Garcia D, Garmendia L, Grande E, Iannirubertо U, Kwiecień A, Leone M, Lignola GP, Lourenço PB, Malena M, Micelli F, Panizza M, Papanicolaou CG, Prota A, Sacco E, Triantafillou TC, Viskovic A, Zając B, Zuccarino G (2012) Round Robin test for composite-to-brick shear bond characterization. RILEM Mater Struct 45(12):1761-1791

Valluzzi MR, Valdemarca M, Modena C (2001) Behavior of brick masonry vaults strengthened by FRP laminates. ASCE J Compos Constr (5)3:163-169

LIST OF FIGURE CAPTIONS

LIST OF TABLE CAPTIONS